Mathematics

https://www.aimspress.com/journal/Math

AIMS Mathematics, 11(9): 28121–28160.
DOI: 10.3934/math.20261122
Received: 05 July 2026
Revised: 20 August 2026
Accepted: 25 August 2026
Published: 03 September 2026

Research article

The Poisson two-sum XLindley distribution: Statistical properties, estimation, regression modeling, and applications

Hanan Haj Ahmad[1,*] **and Mahmoud M. El-Awady**[2]

[1] Department of Mathematics and Statistics, College of Science, King Faisal University, Hofuf 31982, Al-Ahsa, Saudi Arabia

[2] Basic Sciences Department, Misr Higher Institute for Commerce and Computers, Mansoura, Egypt

* **Correspondence:** Email: hhajahmed@kfu.edu.sa.

Abstract: This paper introduces a new one-parameter count model, called the Poisson two-sum XLindley (PTS-XL) distribution, obtained by compounding the Poisson distribution with the two-sum XLindley distribution, defined as the sum of two independent XLindley random variables with a common parameter. The PTS-XL distribution provides a flexible framework for modeling overdispersed and positively skewed data. Several mathematical and statistical properties of the proposed models are derived. Different estimation procedures are developed to estimate the model's parameter, and the performance of the estimators is assessed through simulation studies. Furthermore, a count regression model based on the PTS-XL distribution is developed to model count response data in the presence of covariates. The regression parameters are estimated using the maximum likelihood estimate and assessed through a simulation study. The adequacy of the fitted model is assessed using residual analysis. Finally, real count datasets are analyzed to evaluate the applicability of the proposed distribution and regression model. The results show that the PTS-XL distribution provides a useful and flexible alternative for modeling overdispersed count data.

Keywords: mixed-Poisson distribution; XLindley distribution; two-sum XLindley distribution; maximum likelihood estimation; count regression; simulation study
Mathematics Subject Classification: 60E05, 62E15, 62F10, 62J12

1. Introduction

Count data arise in many theoretical and practical applications, such as epidemiology, demography, ecology, reliability, risk analysis, medical fields, etc. Poisson and negative binomial (NB) distributions are commonly considered for modeling such data. The Poisson distribution is considered when the data exhibit equidispersion, whereas the NB distribution is commonly used for modeling overdispersed data. In practical applications, count data may exhibit high skewness, heavy-tailed behavior, or excess kurtosis. These features are not adequately modeled by Poisson or NB distributions; therefore, considerable attention has been devoted to developing more flexible count distributions to overcome these limitations. Compounding the Poisson distribution with a continuous mixing distribution has become one of the most widely used methods for constructing flexible count models, leading to the class of mixed Poisson distributions; more details can be found in [1].

Various mixed Poisson distributions have been proposed using different continuous mixing distributions, including the Poisson–Lindley distribution [2], the Poisson–Weibull distribution [3], the Poisson quasi–Lindley distribution [4], the Poisson–XLindley distribution [5], the Poisson Xgamma distribution [6], the generalized Poisson model proposed by [7], and the Poisson Mgamma distribution [8], among others.

On the other hand, count regression models are used to study the effect of explanatory variables on the response count variable. The standard choice for modeling count responses is the Poisson regression model, while the NB regression model is used whenever overdispersion exists. Following this, several count regression models have been proposed to relate the mean response to the covariate information and model model overdispersion more adequately, including the Poisson inverse Gaussian regression model [9], the NB–Lindley regression model [10], the Poisson–Weibull regression model [11], the Poisson–weighted exponential regression model [12], the generalized Poisson–Lindley regression model [13], the generalized Poisson regression model of [7], the Poisson quasi-XLindley regression model [14], and the Poisson modified quasi-Lindley regression model [15].

Among the continuous distributions used either as mixing distributions or as baseline models for further generalization is the Lindley distribution, originally introduced by Lindley [16]. The Lindley distribution has received considerable attention because of its simple one-parameter structure and greater flexibility compared with the exponential distribution. These attractive features have led to several extensions aimed at improving its distributional characteristics and expanding its range of applications. Examples include the XLindley distribution proposed by Chouia and Zeghdoudi [17], which is obtained as a finite mixture of the exponential and Lindley distributions and has shown improved performance in modeling lifetime data; the record-based transmuted XLindley distribution studied by Mohan et al. [18]; and the recently proposed q-deformed Lindley distribution by El-Awady et al. [19]. Recent developments have further demonstrated the flexibility of XLindley-based and generalized discrete models. Gemeay et al. [20] introduced the power new XLindley distribution, extending the XLindley family to provide additional shape flexibility together with inferential and reliability properties. In the discrete setting, Seghier et al. [7] proposed a generalized Poisson-type distribution for overdispersed count data and developed an associated regression model. More recently, Haddari et al. [21] introduced a flexible two-parameter family of discrete distributions with various distributional properties. These recent contributions illustrate the continuing development of XLindley-based and Poisson-type models for flexible modeling of continuous and discrete data.

The sum and the difference of two independent Lindley random variables with a common parameter were investigated by Chesneau et al. [22]. The two-sum Lindley (2S-L) distribution is obtained through the convolution of two independent Lindley random variables, producing a richer distributional structure without increasing the number of parameters. The 2S-L has also been used as a mixing distribution to propose the Poisson two-sum Lindley (P2S-L) distribution by Chesneau et al. [23], and used as a basis for generating a new count regression model and an integer-valued autoregressive

INAR(1) process. Furthermore, the bivariate Poisson two-sum Lindley distributions together with the associated bivariate integer-valued autoregressive BINAR(1) processes had been proposed by Irshad et al. [24]. These contributions demonstrate that convolution-based Lindley models provide effective mixing distributions for constructing flexible count distributions.

Motivated by the additional flexibility provided by the convolution-based two-sum construction while preserving the one-parameter structure, together with the successful use of the XLindley distribution as a mixing distribution in the mixed Poisson framework, this paper introduces a new one-parameter count distribution, called the Poisson two-sum XLindley (PTS-XL) distribution. Unlike recent continuous extensions of the XLindley family and generalized discrete constructions, the proposed model is obtained by first forming the convolution of two independent XLindley random variables and then using the resulting two-sum XLindley distribution as the mixing distribution of a Poisson model. This construction preserves a parsimonious one-parameter structure while generating a flexible overdispersed count distribution and an associated regression model.

The statistical properties of the PTS-XL distribution are investigated, including its probability function, moments, generating functions, reliability measures, and dispersion characteristics. The estimation of the parameter of the PTS-XL model is obtained using different estimation methods, and its performance is assessed through Monte Carlo simulation. Furthermore, a new count regression model based on the PTS-XL distribution is proposed to analyze overdispersed count data in the presence of covariates. The regression parameters are estimated using the maximum likelihood method, and the performance of the estimators is assessed through simulation. The adequacy of the fitted regression model is evaluated using randomized quantile residuals. Finally, the practical usefulness of the PTS-XL count distribution and its regression model is illustrated using real count data-sets and comparisons with several existing mixed Poisson models.

This work is organized in the following order: Section 2 defines the Poisson two-sum XLindley distribution. The properties of the proposed model and related measures are presented in Section 3. The point estimate of the parameter of the PTS-XL distribution is obtained using different estimation methods in Section 4, while Section 5 discusses obtaining the interval estimation of the parameter. Simulation analysis is explored in Section 6. Regression model formulation and its related analysis and simulation are performed in Section 7. Finally, real data applications are illustrated in Section 8.

2. The Poisson two-sum XLindley distribution

We first define the two-sum XLindley (TS-XL) distribution, which serves as the mixing distribution of the proposed mixed Poisson model. The TS-XL distribution is obtained as the sum of two XLindley (XL) distributions with a common parameter. The probability density function (PDF) and cumulative distribution function (CDF) of the XL distribution are given by

$$f_{XL}(t;\theta) = \frac{\theta^2}{(1+\theta)^2}(2+\theta+t)e^{-\theta t},\ t,\theta > 0 \tag{2.1}$$

and

$$F_{XL}(t;\theta) = 1 - \left(1 + \frac{\theta t}{(1+\theta)^2}\right)e^{-\theta t},\ t,\theta > 0, \tag{2.2}$$

respectively. Suppose Y_1 and Y_2 are independent random variables following the XL distribution with common parameter $\theta > 0$. We define the TS-XL distribution as the distribution of $Y = Y_1 + Y_2$. The

PDF of Y is obtained via convolution as

$$f_Y(y;\theta) = \int_0^y f_{XL}(t;\theta) f_{XL}(y-t;\theta)\,dt, \quad y > 0. \tag{2.3}$$

Substituting the PDF of XL distribution in (2.1) gives

$$f_Y(y;\theta) = \frac{\theta^4 e^{-\theta y}}{(1+\theta)^4}\int_0^y (2+\theta+t)(2+\theta+y-t)\,dt. \tag{2.4}$$

Direct evaluation of the integral leads to the PDF of the TS-XL distribution as follows:

$$f_Y(y;\theta) = \frac{\theta^4 y e^{-\theta y}}{(1+\theta)^4}\left(\frac{y^2}{6} + (2+\theta)y + (2+\theta)^2\right), \quad y > 0. \tag{2.5}$$

The corresponding CDF of the TS-XL distribution is obtained by (2.5) as

$$\begin{aligned} F_Y(y;\theta) &= \int_0^y f_Y(t;\theta)\,dt \\ &= \frac{\theta^4}{(1+\theta)^4}\int_0^y te^{-\theta t}\left(\frac{t^2}{6} + (2+\theta)t + (2+\theta)^2\right)dt, \end{aligned} \tag{2.6}$$

which yields

$$F_Y(y;\theta) = 1 - \frac{e^{-\theta y}}{(1+\theta)^4}\left[(1+\theta)^4 + \theta(1+\theta)^4 y + \frac{\theta^2}{2}(2\theta^2+4\theta+1)y^2 + \frac{\theta^3}{6}y^3\right], \quad y > 0. \tag{2.7}$$

The TS-XL distribution inherits flexibility from the XLindley model while introducing additional variability through convolution. Motivated by these features, we use the TS-XL distribution as a mixing distribution for the Poisson parameter. The probability mass function (PMF) for the Poisson distribution is

$$P(X = x \mid \lambda) = \frac{e^{-\lambda}\lambda^x}{x!}, \tag{2.8}$$

where $x = 0, 1, 2, \ldots$ and $\lambda > 0$. Suppose that the Poisson rate parameter λ follows the TS-XL distribution with parameter θ, $\lambda \sim$ TS-XL(θ), then the resulting mixed Poisson model is called the PTS-XL distribution. The following proposition proposes the PMF for the PTS-XL distribution.

Proposition 1. Let $X \mid \lambda \sim$ Poisson(λ), where $\lambda \sim$ TS-XL(θ). Then the unconditional PMF of X is

$$p_X(x;\theta) = \frac{\theta^4(1+x)}{6(1+\theta)^{x+8}}\left[x^2 + x\left(17 + 6\theta(\theta+3)\right) + 6(3+\theta(\theta+3))^2\right], \tag{2.9}$$

where $x = 0, 1, 2, \ldots,$ and $\theta > 0$.

Proof. The marginal PMF of X is obtained by integrating the conditional Poisson probability over the density of λ, i.e.,

$$p_X(x;\theta) = \int_0^\infty P(X = x \mid \lambda) f_\lambda(\lambda;\theta)\,d\lambda.$$

Substituting Eqs (2.5) and (2.8) into the above integral gives

$$p_X(x;\theta) = \frac{\theta^4}{x!(1+\theta)^4}\int_0^\infty \lambda^x e^{-(1+\theta)\lambda}\left(\frac{\lambda^3}{6} + (2+\theta)\lambda^2 + (2+\theta)^2\lambda\right)d\lambda.$$

Applying the gamma integral $\int_0^\infty \lambda^m e^{-a\lambda}d\lambda = \frac{\Gamma(m+1)}{a^{m+1}}, \quad a>0, m>-1$, we obtain

$$p_X(x;\theta) = \frac{\theta^4}{x!(1+\theta)^4}\left[\frac{\Gamma(x+4)}{6(1+\theta)^{x+4}} + (2+\theta)\frac{\Gamma(x+3)}{(1+\theta)^{x+3}} + (2+\theta)^2\frac{\Gamma(x+2)}{(1+\theta)^{x+2}}\right].$$

The previous expression can be rewritten as

$$\begin{aligned} p_X(x;\theta) &= \frac{\theta^4(1+x)}{6(1+\theta)^{x+8}}\left[(x+2)(x+3) + 6(2+\theta)(1+\theta)(x+2) + 6(2+\theta)^2(1+\theta)^2\right] \\ &= \frac{\theta^4(1+x)}{6(1+\theta)^{x+8}}\left[x^2 + x\left(17+6\theta(\theta+3)\right) + 6\left(3+\theta(\theta+3)\right)^2\right]. \end{aligned}$$

This completes the proof. □

Figure 1 illustrates the behavior of the PMF of the PTS-XL distribution for selected values of θ. In general, the distribution is right-skewed and unimodal, as established in Theorem 3.1. It can be observed that the tail behavior of the distribution varies with the parameter, allowing different levels of dispersion. This indicates that the PTS-XL distribution accommodates different count-data patterns.

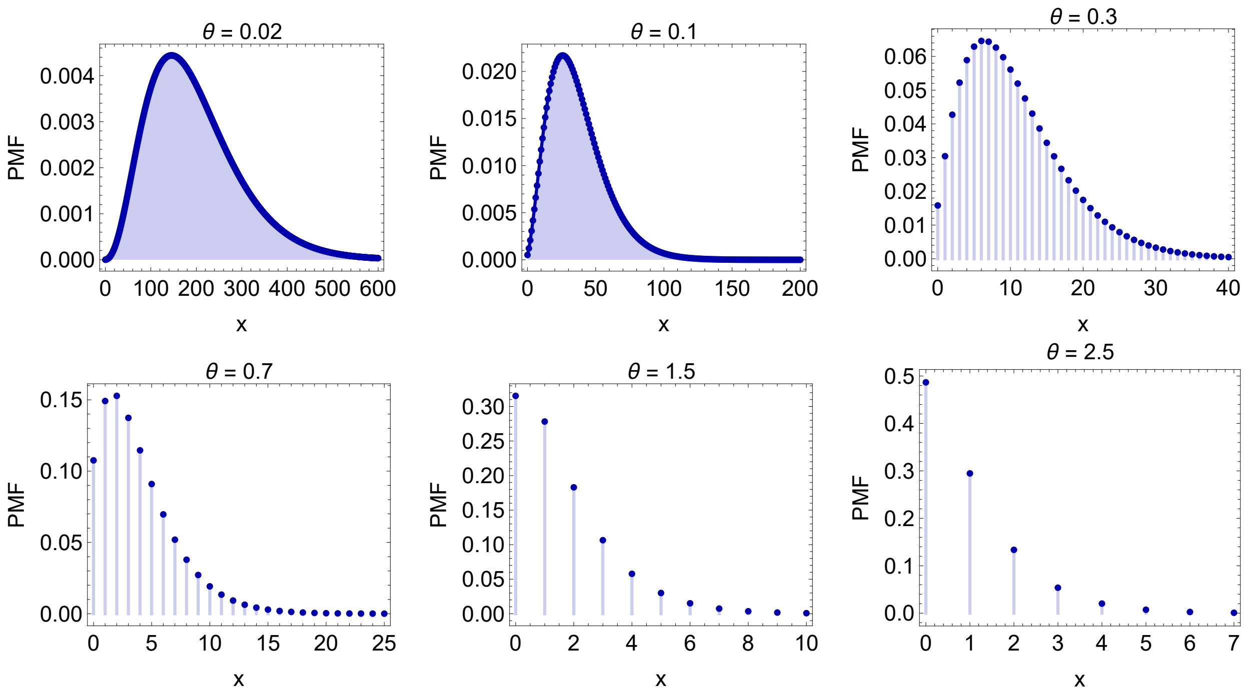

Figure 1. PMF of the PTS-XL distribution for selected values of θ.

The CDF for the PTS-XL distribution is defined as $F_X(x;\theta) = 1 - S_X(x;\theta)$, where $S_X(x;\theta) = \sum_{t=x+1}^{\infty} p_X(t;\theta)$ is the survival function (SF), and $p_X(t;\theta)$ is given in (2.9). The closed-form expression for $S_X(x;\theta)$ is obtained by applying the standard finite-tail sums of polynomial-geometric series as follows:

$$\sum_{t=x+1}^{\infty} q^t = \frac{q^{x+1}}{1-q}, \ \sum_{t=x+1}^{\infty} tq^t = \frac{q^{x+1}\{x+1-xq\}}{(1-q)^2}, \ \text{and} \ \sum_{t=x+1}^{\infty} t^2 q^t = \frac{q^{x+1}\{(x+1)^2-(2x^2+2x-1)q+x^2q^2\}}{(1-q)^3}.$$

Substituting $q = (1+\theta)^{-1}$, the SF reduces to

$$S_X(x;\theta) = \frac{1}{6}(1+\theta)^{-x-8}\left[\omega_0(\theta)+\omega_1(\theta)x+\omega_2(\theta)x^2+\theta^3x^3\right], \tag{2.10}$$

where

$$\begin{aligned}\omega_0(\theta) &= 6(\theta^3+3\theta^2+4\theta+1)(2\theta^4+7\theta^3+9\theta^2+4\theta+1),\\ \omega_1(\theta) &= \theta^7+6\theta^6+18\theta^5+87\theta^4+146\theta^3+45\theta^2+6\theta,\\ \omega_2(\theta) &= 3\theta^2\left(2\theta^3+6\theta^2+7\theta+1\right).\end{aligned}$$

Hence, the CDF of the PTS-XL distribution is

$$F_X(x;\theta) = 1-\frac{1}{6}(1+\theta)^{-x-8}\left[\omega_0(\theta)+\omega_1(\theta)x+\omega_2(\theta)x^2+\theta^3x^3\right]. \tag{2.11}$$

The hazard function (or failure rate) of the PTS-XL distribution is defined as

$$h_X(x;\theta) = \frac{p_X(x;\theta)}{P(X\geq x;\theta)} = \frac{p_X(x;\theta)}{S_X(x-1;\theta)}, \qquad x = 0,1,2,\ldots. \tag{2.12}$$

Using the PMF in (2.9) and the SF in (2.10), the hazard function reduces to

$$h_X(x;\theta) = \frac{\theta^4(x+1)}{1+\theta}\,\frac{x^2+x\{17+6\theta(\theta+3)\}+6\{3+\theta(\theta+3)\}^2}{\omega_0(\theta)+\omega_1(\theta)(x-1)+\omega_2(\theta)(x-1)^2+\theta^3(x-1)^3}, \qquad x=0,1,2,\ldots,\ \theta>0, \tag{2.13}$$

where ω_0, ω_1, and ω_2 are defined in (2.10).

Figure 2 displays the hazard function (HF) of the PTS-XL distribution for selected values of θ. The plots show that the HF is increasing in x for all displayed parameter values, as established in Corollary 1 in the next section.

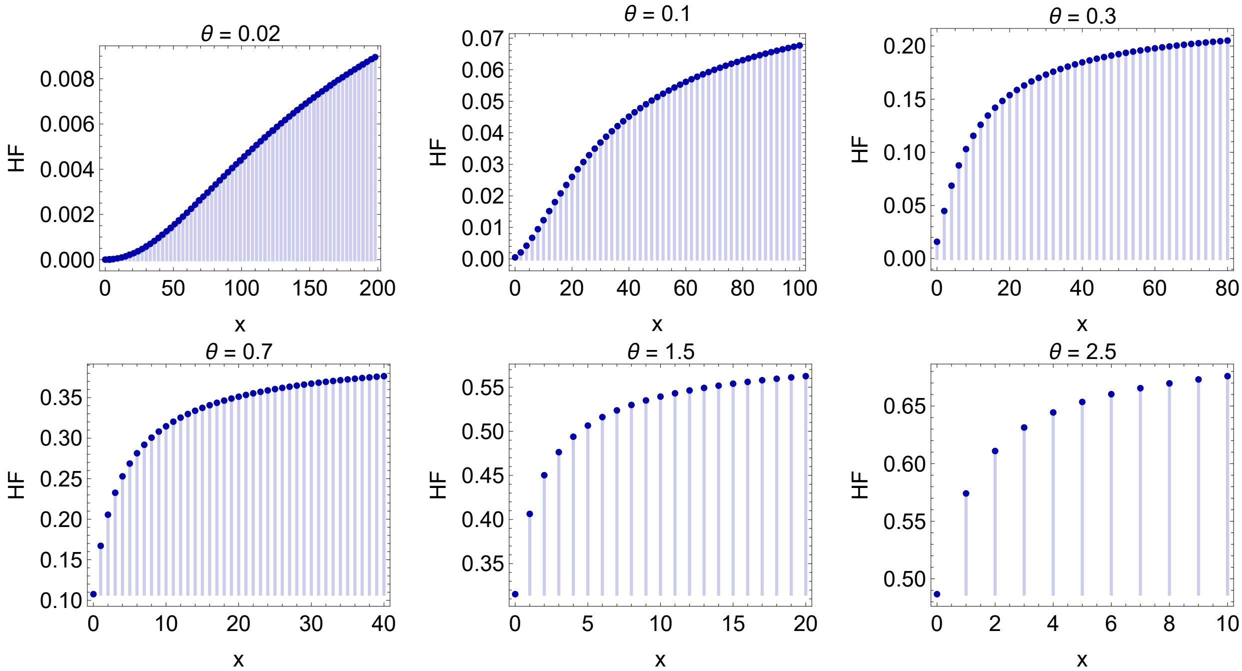

Figure 2. The HF of the PTS-XL distribution for selected values of θ.

3. Properties

This section investigates the main distributional properties of the PTS-XL distribution.

3.1. Analytical behavior of PMF and HF

The limiting behavior of the PMF and HF of the PTS-XL distribution are discussed in this subsection. From the PMF in (2.9), the highest-degree term in the polynomial factor is x^3. Hence, for a large x, we have

$$p_x \sim \frac{\theta^4 x^3}{6(1+\theta)^{x+8}}, \qquad x \to \infty.$$

This implies that as x tends to ∞ the PMF tends to 0. Similarly, from the SF in (2.10), the leading term of the polynomial is $\theta^3 x^3$, giving

$$S_x \sim \frac{\theta^3 x^3}{6(1+\theta)^{x+7}}, \qquad x \to \infty.$$

By the HF definition $h_X(x;\theta) = p_x/S_{x-1}$, and noting that $S_{x-1} \sim (1+\theta)S_x$ asymptotically, we obtain

$$\lim_{x\to\infty} h_X(x;\theta) = \lim_{x\to\infty} \frac{p_x}{S_{x-1}} = \frac{\theta}{1+\theta}.$$

Thus, the HF approaches a finite horizontal asymptote as $x \to \infty$, with the limiting value $\theta/(1+\theta)$. At the lower boundary, the hazard rate starts from

$$h_X(0;\theta) = \frac{\theta^4(\theta(\theta+3)+3)^2}{(1+\theta)^8}.$$

3.2. Log-concavity

To investigate the behavior of the PMF of the PTS-XL distribution, we need to examine the ratio of successive probabilities $\frac{p_X(x+1;\theta)}{p_X(x;\theta)}$. The following theorem establishes the log-concavity of the PMF in (2.9).

Theorem 3.1. *Let X follow the PTS-XL distribution with the PMF given in Eq* (2.9)*, and let*

$$p_x = p_X(x;\theta), \qquad x = 0, 1, 2, \ldots.$$

Then the sequence $\{p_x\}_{x\geq 0}$ is strictly log-concave. Consequently, the PTS-XL distribution is unimodal.

Proof. Using the PMF in Eq (2.9), the ratio of two successive probabilities is

$$R_x = \frac{p_{x+1}}{p_x} = \frac{x+2}{(1+\theta)(x+1)} \frac{A_\theta(x+1)}{A_\theta(x)}, \qquad x = 0, 1, 2, \ldots,$$

where $A_\theta(x) = x^2 + x\,[17 + 6\theta(\theta+3)] + 6\,[3 + \theta(\theta+3)]^2$. To establish log-concavity, it is sufficient to prove that R_x is decreasing in x. Direct algebra gives

$$R_x - R_{x+1} = \frac{3H_\theta(x)}{(1+\theta)(x+1)(x+2)A_\theta(x)A_\theta(x+1)},$$

where

$$\begin{aligned} H_\theta(x) = {} & x^4 + 28x^3 + 293x^2 + 1238x + 1944 \\ & + \theta\left(24x^3 + 504x^2 + 3072x + 6480\right) \\ & + \theta^2\left(8x^3 + 384x^2 + 3508x + 10260\right) \\ & + \theta^3\left(144x^2 + 2304x + 9936\right) \\ & + \theta^4\left(24x^2 + 924x + 6408\right) \\ & + \theta^5\,(216x + 2808) \\ & + \theta^6\,(24x + 816) + 144\theta^7 + 12\theta^8. \end{aligned}$$

For $x \geq 0$ and $\theta > 0$, every term in $H_\theta(x)$ is positive. Since the denominator is positive for all $x \geq 0$ and $\theta > 0$, we have $R_x - R_{x+1} > 0$. Thus, the successive probability ratio R_x is strictly decreasing, which implies

$$\frac{p_{x+1}}{p_x} > \frac{p_{x+2}}{p_{x+1}},$$

or equivalently

$$p_{x+1}^2 > p_x p_{x+2}.$$

Thus, the PMF is strictly log-concave. Since every positive log-concave probability sequence is unimodal, the PTS-XL distribution is unimodal [25]. □

It is well established that a log-concave PMF possesses the discrete increasing failure rate (IFR) property [26]. Therefore, as an immediate consequence of the strict log-concavity established in Theorem 3.1, the following result is obtained.

Corollary 1. *The HF of the PTS-XL distribution given in Eq* (2.13) *is increasing in x. Hence, the PTS-XL distribution possesses the discrete IFR property.*

The IFR property implies several important aging properties of discrete lifetime distributions. In particular, the standard hierarchy of reliability classes gives

$$\text{IFR} \Rightarrow \text{IFRA} \Rightarrow \text{NBU} \Rightarrow \text{NBUE} \Rightarrow \text{DMRL},$$

where IFRA denotes the increasing failure rate average, NBU denotes new better than used, NBUE denotes new better than used in expectation, and DMRL denotes decreasing mean residual lifetime [27]. Therefore, the following result follows directly.

Corollary 2. *The PTS-XL distribution possesses the IFRA, NBU, NBUE, and DMRL properties.*

3.3. Moments and related measures

The factorial moments play an important role in studying count distributions, particularly regarding dispersion and generating functions. For the PTS-XL distribution, the factorial moments are

$$\mu'_{[r]} = E[X(X-1)\cdots(X-r+1)], \qquad r = 1, 2, \ldots. \tag{3.1}$$

Since the PTS-XL distribution is obtained as a mixed Poisson distribution with mixing variable $\lambda \sim$ TS-XL(θ), its factorial moments can be obtained directly using the well-known property of mixed Poisson distributions:

$$\mu'_{[r]} = E(\lambda^r). \tag{3.2}$$

Therefore, the problem reduces to evaluating the rth raw moment of the TS-XL distribution. Using the density of the TS-XL distribution, we have

$$\mu'_{[r]} = \int_0^\infty \lambda^r f_\lambda(\lambda;\theta)\, d\lambda. \tag{3.3}$$

Substituting the PDF of (2.5) of the TS-XL yields

$$\mu'_{[r]} = \frac{\theta^4}{(1+\theta)^4}\int_0^\infty \lambda^{r+1}\left(\frac{\lambda^2}{6} + (2+\theta)\lambda + (2+\theta)^2\right)e^{-\theta\lambda}d\lambda. \tag{3.4}$$

Applying the gamma integral $\int_0^\infty \lambda^m e^{-\theta\lambda}d\lambda = \frac{\Gamma(m+1)}{\theta^{m+1}}$, gives

$$\begin{aligned}
\mu'_{[r]} &= \frac{\theta^4}{(1+\theta)^4}\left[\frac{1}{6}\int_0^\infty \lambda^{r+3}e^{-\theta\lambda}d\lambda + (2+\theta)\int_0^\infty \lambda^{r+2}e^{-\theta\lambda}d\lambda + (2+\theta)^2\int_0^\infty \lambda^{r+1}e^{-\theta\lambda}d\lambda\right] \\
&= \frac{\theta^4}{(1+\theta)^4}\left[\frac{\Gamma(r+4)}{6\theta^{r+4}} + (2+\theta)\frac{\Gamma(r+3)}{\theta^{r+3}} + (2+\theta)^2\frac{\Gamma(r+2)}{\theta^{r+2}}\right].
\end{aligned}$$

We obtain

$$\mu'_{[r]} = \frac{(r+1)!}{6(1+\theta)^4\theta^r}\left[(r+2)(r+3) + 6\theta(2+\theta)(r+2) + 6\theta^2(2+\theta)^2\right].$$

After expanding and collecting the terms in r, this becomes

$$\mu'_{[r]} = \frac{(r+1)!}{6(1+\theta)^4\,\theta^r}\left[r^2 + 6(\theta+1)^4 + r(5+6\theta(\theta+2))\right]. \tag{3.5}$$

The ordinary raw moments can be expressed in terms of factorial moments through the Stirling numbers of the second kind: $\mu'_r = E(X^r) = \sum_{k=1}^{r} S(r,k)\,\mu'_{[k]}$. Hence, the first four ordinary raw moments of X are obtained as

$$\mu'_1 = E(X) = \mu'_{[1]} = \frac{4+2\theta(2+\theta)}{\theta(1+\theta)^2}, \tag{3.6}$$

$$\mu'_2 = E(X^2) = \mu'_{[1]} + \mu'_{[2]} = \frac{2\theta^5 + 14\theta^4 + 38\theta^3 + 60\theta^2 + 52\theta + 20}{\theta^2(1+\theta)^4}, \tag{3.7}$$

$$\mu'_3 = E(X^3) = \mu'_{[1]} + 3\mu'_{[2]} + \mu'_{[3]} = \frac{2\theta^6 + 26\theta^5 + 110\theta^4 + 252\theta^3 + 364\theta^2 + 300\theta + 120}{\theta^3(1+\theta)^4}, \tag{3.8}$$

$$\begin{aligned}\mu'_4 = E(X^4) &= \mu'_{[1]} + 7\mu'_{[2]} + 6\mu'_{[3]} + \mu'_{[4]} \\ &= \frac{2\theta^7 + 50\theta^6 + 326\theta^5 + 1044\theta^4 + 2116\theta^3 + 2780\theta^2 + 2160\theta + 840}{\theta^4(1+\theta)^4}.\end{aligned} \tag{3.9}$$

The corresponding central moments are

$$\mu_1 = E(X - E(X)) = 0, \tag{3.10}$$

$$\mu_2 = Var(X) = \mu'_2 - (\mu'_1)^2 = \frac{2\left(\theta^5 + 5\theta^4 + 11\theta^3 + 14\theta^2 + 10\theta + 2\right)}{\theta^2(1+\theta)^4}, \tag{3.11}$$

$$\begin{aligned}\mu_3 &= \mu'_3 - 3\mu'_2\mu'_1 + 2(\mu'_1)^3 \\ &= \frac{2(\theta+2)\left(\theta^7 + 7\theta^6 + 22\theta^5 + 43\theta^4 + 55\theta^3 + 42\theta^2 + 14\theta + 2\right)}{\theta^3(1+\theta)^6},\end{aligned} \tag{3.12}$$

$$\begin{aligned}\mu_4 &= \mu'_4 - 4\mu'_3\mu'_1 + 6\mu'_2(\mu'_1)^2 - 3(\mu'_1)^4 \\ &= \frac{2\left(\theta^7 + 17\theta^6 + 83\theta^5 + 218\theta^4 + 370\theta^3 + 398\theta^2 + 216\theta + 36\right)}{\theta^4(1+\theta)^4}.\end{aligned} \tag{3.13}$$

To verify the symbolic expressions presented throughout the paper, the defining expressions were evaluated numerically for several values of θ and compared with the corresponding closed-form expressions. The dispersion index (DI), defined as the ratio of the variance to the mean, provides a simple and informative measure of the variability exhibited by count data. An index smaller than one indicates underdispersion and a value greater than one signifies overdispersion. The DI for the PTS-XL distribution is expressed as

$$\mathrm{DI} = \frac{\theta^5 + 5\theta^4 + 11\theta^3 + 14\theta^2 + 10\theta + 2}{\theta(1+\theta)^2(\theta^2 + 2\theta + 2)}. \tag{3.14}$$

Additionally, closed-form expressions for the skewness and kurtosis can be obtained from

$$\text{Skewness} = \frac{\mu_3' - 3\mu_2'\mu_1' + 2(\mu_1')^3}{\left(\mu_2' - (\mu_1')^2\right)^{3/2}}, \qquad \text{and} \qquad \text{Kurtosis} = \frac{\mu_4' - 4\mu_3'\mu_1' + 6\mu_2'(\mu_1')^2 - 3(\mu_1')^4}{\left(\mu_2' - (\mu_1')^2\right)^2}.$$

For further investigation of the distributional properties of the PTS-XL distribution, the first three raw moments along with the variance, DI, skewness, and kurtosis are listed in Table 1 for different values of the parameter θ. The results in the table indicate that the first three raw moments and the variance decrease monotonically as θ increases. The DI approaches unity as θ increases, indicating that the PTS-XL distribution can be used to model data with dispersion levels ranging from overdispersion, moderate, and equidispersion. The PTS-XL distribution is right skewed, as the values of the skewness are positive and exhibit an increasing trend as θ increases. Similarly, the kurtosis coefficient increases with θ, indicating the heavy-tailed nature of the PTS-XL distribution.

Table 1. Moments and related measures of the PTS-XL distribution for different values of θ.

θ	μ_1'	μ_2'	μ_3'	Variance	DI	Skewness	Kurtosis
0.1	36.529	1764.9	105118.0	430.50	11.785	1.0297	4.5678
0.25	13.120	245.11	5823.3	72.973	5.5620	1.1113	4.7887
0.5	5.7778	52.691	632.44	19.309	3.3419	1.2362	5.1921
0.75	3.5374	21.549	176.26	9.0359	2.5544	1.3291	5.5289
1	2.5000	11.625	73.375	5.3750	2.1500	1.3993	5.7934
1.25	1.9160	7.3230	38.1862	3.6518	1.9059	1.4560	6.0058
1.5	1.5467	5.0894	22.881	2.6972	1.7439	1.5049	6.1847
2	1.1111	2.9506	10.667	1.7160	1.5444	1.5902	6.4876
2.5	0.8653	1.9842	6.1443	1.2354	1.4277	1.6672	6.7571
3	0.7083	1.4592	4.0200	0.9575	1.3517	1.7398	7.0136
4	0.5200	0.9252	2.1562	0.6548	1.2592	1.8762	7.5148
5	0.4111	0.6645	1.3794	0.4955	1.2053	2.0037	8.0123
6	0.3401	0.5136	0.9786	0.3979	1.1699	2.1239	8.5099
7	0.2902	0.4165	0.7423	0.3323	1.1450	2.2380	9.0079
8	0.2531	0.3492	0.5899	0.2851	1.1265	2.3467	9.5064
9	0.2244	0.3000	0.4850	0.2496	1.1122	2.4506	10.0053
10	0.2017	0.2626	0.4092	0.2220	1.1008	2.5504	10.5044
50	0.0400	0.0424	0.0474	0.0408	1.0200	5.1478	30.5002
100	0.0200	0.0206	0.0218	0.0202	1.0100	7.1764	55.5000

3.4. Probability-generating function

The probability-generating function (PGF) is a fundamental tool in the study of discrete distributions, as it characterizes the distribution and facilitates the derivation of several of its properties.

The following proposition provides a closed-form expression for the PGF of the PTS-XL distribution.
Proposition 2. Let X follows the PTS–XL with the parameter $\theta > 0$, then the PGF of X is given by

$$G_X(z) = \frac{\theta^4 \left[\theta^2 + 3\theta + 3 - (\theta + 2)z\right]^2}{(1+\theta)^4(1+\theta-z)^4}, \qquad |z| < 1 + \theta. \tag{3.15}$$

Proof. By definition, $G_X(z) = E(z^X) = \sum_{x=0}^{\infty} z^x p_X(x;\theta)$. Using the PMF of the PTS-XL distribution in (2.9), we obtain

$$G_X(z) = \sum_{x=0}^{\infty} z^x \frac{\theta^4(1+x)}{6(1+\theta)^{x+8}} \left[x^2 + x\{17 + 6\theta(\theta+3)\} + 6\{3 + \theta(\theta+3)\}^2\right].$$

Let $r = \frac{z}{1+\theta}$, the series converges whenever $|r| < 1$ or, equivalently, $|z| < 1 + \theta$. Hence, we have

$$G_X(z) = \frac{\theta^4}{6(1+\theta)^8} \sum_{x=0}^{\infty} r^x \Big[x^3 + \{18 + 6\theta(\theta+3)\}x^2 + \{17 + 6\theta(\theta+3) + 6[3+\theta(\theta+3)]^2\}x + 6[3+\theta(\theta+3)]^2\Big].$$

Using the following standard power series identities, we have

$$\sum_{x=0}^{\infty} r^x = \frac{1}{1-r}, \ \sum_{x=0}^{\infty} x r^x = \frac{r}{(1-r)^2}, \ \sum_{x=0}^{\infty} x^2 r^x = \frac{r(1+r)}{(1-r)^3}, \text{ and } \sum_{x=0}^{\infty} x^3 r^x = \frac{r(1+4r+r^2)}{(1-r)^4},$$

we get

$$\begin{aligned} G_X(z) = \frac{\theta^4}{6(1+\theta)^8} \Bigg[& \frac{r(1+4r+r^2)}{(1-r)^4} + \{18 + 6\theta(\theta+3)\}\frac{r(1+r)}{(1-r)^3} \\ & + \{17 + 6\theta(\theta+3) + 6[3+\theta(\theta+3)]^2\}\frac{r}{(1-r)^2} + 6[3+\theta(\theta+3)]^2 \frac{1}{1-r}\Bigg]. \end{aligned}$$

Substituting $r = z/(1+\theta)$, collecting the terms over the common denominator $(1-r)^4$, and then replacing $1 - r$ by $(1 + \theta - z)/(1 + \theta)$, we obtain Eq (3.15).

3.5. Moment-generating function

The moment-generating function (MGF) provides an alternative characterization of the distribution and is useful for deriving moments and other analytical properties. The following proposition gives its closed-form expression for the PTS-XL distribution.
Proposition 3. Let X follows the PTS-XL distribution with parameter $\theta > 0$, then the MGF of X is given by

$$M_X(t) = E(e^{tX}) = \frac{\theta^4}{(1+\theta)^4} \frac{\left[\theta^2 + 3\theta + 3 - (\theta+2)e^t\right]^2}{(1+\theta-e^t)^4}, \qquad t < \log(1+\theta). \tag{3.16}$$

Proof. By definition, the MGF is $M_X(t) = E(e^{tX})$. From the PGF of the PTS-XL distribution in (3.15) the MGF follows immediately by substituting $z = e^t$. Therefore, we have

$$M_X(t) = G_X(e^t) = \frac{\theta^4}{(1+\theta)^4} \frac{\left[\theta^2 + 3\theta + 3 - (\theta+2)e^t\right]^2}{(1+\theta-e^t)^4}.$$

Since the MGF of a discrete random variable is related to the PGF by $M_X(t) = G_X(e^t)$, the domain condition $|z| < 1 + \theta$ becomes $e^t < 1 + \theta$ or, equivalently, $t < \log(1 + \theta)$.

3.6. Stress–strength reliability

The stress–strength reliability parameter is an important measure in reliability analysis. It measures the probability that the strength (Y) of a component exceeds the applied stress (X). Consider that X and Y be two independent random variables following the PTS-XL distribution with parameters θ_1 and θ_2, respectively; then the stress–strength reliability is

$$R = P(X < Y) = \sum_{x=0}^{\infty} p_X(x;\theta_1)\left[1 - F_Y(x;\theta_2)\right].$$

Using the PMF in (2.9) and the CDF in (2.11), we have

$$\begin{aligned} R = &\frac{\theta_1^4}{36(1+\theta_1)^8(1+\theta_2)^8} \sum_{x=0}^{\infty} \left[\frac{1}{(1+\theta_1)(1+\theta_2)}\right]^x (x+1) \\ &\times \left[x^2 + x\{17 + 6\theta_1(\theta_1+3)\} + 6\{3 + \theta_1(\theta_1+3)\}^2\right] \\ &\times \left[\omega_0(\theta_2) + \omega_1(\theta_2)x + \omega_2(\theta_2)x^2 + \theta_2^3 x^3\right]. \end{aligned}$$

Let $q = \frac{1}{(1+\theta_1)(1+\theta_2)}$, where $0 < q < 1$ for all $\theta_1, \theta_2 > 0$. The summand is the product of a sixth-degree polynomial in x and the geometric sequence q^x. Expanding the polynomial product and collecting like powers of x yield

$$R = \frac{\theta_1^4}{36(1+\theta_1)^8(1+\theta_2)^8} \sum_{j=0}^{6} c_j G_j(q), \tag{3.17}$$

where $G_j(q) = \sum_{x=0}^{\infty} x^j q^x$, $j = 0, 1, \ldots, 6$, and the coefficients c_j are

$$\begin{aligned} c_0 &= \mathcal{B}\omega_0, \\ c_1 &= \mathcal{B}\omega_1 + (\mathcal{A}+\mathcal{B})\omega_0, \\ c_2 &= \mathcal{B}\omega_2 + (\mathcal{A}+\mathcal{B})\omega_1 + (\mathcal{A}+1)\omega_0, \\ c_3 &= \mathcal{B}\theta_2^3 + (\mathcal{A}+\mathcal{B})\omega_2 + (\mathcal{A}+1)\omega_1 + \omega_0, \\ c_4 &= (\mathcal{A}+\mathcal{B})\theta_2^3 + (\mathcal{A}+1)\omega_2 + \omega_1, \\ c_5 &= (\mathcal{A}+1)\theta_2^3 + \omega_2, \\ c_6 &= \theta_2^3 \end{aligned}$$

with $\mathcal{A} = 17 + 6\theta_1(\theta_1+3)$, $\mathcal{B} = 6\{3 + \theta_1(\theta_1+3)\}^2$, and $\omega_i; i = 1, 2, 3$, are given in Eq (2.10), evaluated at $\theta = \theta_1$. For the power sum $G_j(q)$, we have

$$G_j(q) = \begin{cases} \dfrac{1}{1-q}, & j = 0, \\ \mathrm{Li}_{-j}(q), & j = 1, \ldots, 6, \end{cases}$$

where $\mathrm{Li}_{-j}(q)$ is the polylogarithm function defined in [28, Eq (25.12.10)] can be evaluated directly in Mathematica using the built-in function PolyLog$[-j, q]$. Figure 3 displayed the behavior of the stress–strength reliability for different values of θ_1 and θ_2.

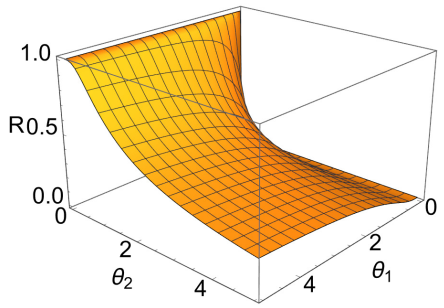

Figure 3. The stress–strength reliability of the PTS-XL distribution for different values of θ_1 and θ_2.

Table 2. Summary of the main properties of the PTS-XL distribution.

Property	**Expression/result**	**Reference**
PMF	$p_X(x;\theta) = \frac{\theta^4(1+x)}{6(1+\theta)^{x+8}}\left[x^2 + x\{17 + 6\theta(\theta+3)\} + 6\{3 + \theta(\theta+3)\}^2\right]$, $x = 0, 1, 2, \ldots,\ \theta > 0$	Eq (2.9)
SF	$S_X(x;\theta) = \frac{(1+\theta)^{-x-8}}{6}\left[\omega_0(\theta) + \omega_1(\theta)x + \omega_2(\theta)x^2 + \theta^3 x^3\right]$	Eq (2.10)
CDF	$F_X(x;\theta) = 1 - S_X(x;\theta)$	Eq (2.11)
HF	$h_X(x;\theta) = \frac{\theta^4(x+1)}{1+\theta}\frac{x^2+x\{17+6\theta(\theta+3)\}+6\{3+\theta(\theta+3)\}^2}{\omega_0(\theta)+\omega_1(\theta)(x-1)+\omega_2(\theta)(x-1)^2+\theta^3(x-1)^3}$	Eq (2.13)
Asymptotic behavior of PMF	$p_X(x;\theta) \sim \dfrac{\theta^4 x^3}{6(1+\theta)^{x+8}}, \quad x \to \infty$	Subsection 3.1
Limiting HF	$\lim\limits_{x\to\infty} h_X(x;\theta) = \dfrac{\theta}{1+\theta}$	Subsection 3.1
Log-concavity and unimodality	The PMF is strictly log-concave for all $\theta > 0$; consequently, the PTS-XL distribution is unimodal.	Theorem 3.1
HF behavior	$h_X(x;\theta)$ is increasing in x and θ.	Corollary 1
Factorial moments	$\mu'_{[r]} = \frac{(r+1)!}{6(1+\theta)^4\theta^r}\left[r^2 + 6(1+\theta)^4 + r\{5 + 6\theta(\theta+2)\}\right]$	Eq (3.5)
Mean	$E(X) = \frac{4+2\theta(2+\theta)}{\theta(1+\theta)^2}$	Eq (3.6)
Variance	$\mathrm{Var}(X) = \frac{2(\theta^5+5\theta^4+11\theta^3+14\theta^2+10\theta+2)}{\theta^2(1+\theta)^4}$	Eq (3.11)
Dispersion index	$DI = \frac{\theta^5+5\theta^4+11\theta^3+14\theta^2+10\theta+2}{\theta(1+\theta)^2(\theta^2+2\theta+2)}$	Eq (3.14)
PGF	$G_X(z) = \frac{\theta^4[\theta^2+3\theta+3-(\theta+2)z]^2}{(1+\theta)^4(1+\theta-z)^4}, \qquad \lvert z\rvert < 1+\theta$	Eq (3.15)
MGF	$M_X(t) = \frac{\theta^4[\theta^2+3\theta+3-(\theta+2)e^t]^2}{(1+\theta)^4(1+\theta-e^t)^4}, \qquad t < \log(1+\theta)$	Eq (3.16)
Stress–strength reliability	$R = P(X < Y) = \frac{\theta_1^4}{36(1+\theta_1)^8(1+\theta_2)^8}\sum_{j=0}^{6} c_j G_j(q),\ q = \frac{1}{(1+\theta_1)(1+\theta_2)}$	Eq (3.17)

For convenient reference, Table 2 summarizes the principal theoretical properties of the proposed PTS-XL distribution. The table is intended to provide a concise overview, while the corresponding derivations and proofs are given in the preceding subsections.

4. Point estimation

Statistical inference for parametric probability models can be conducted through several approaches, including moment-based, likelihood-based, least-squares, and Bayesian procedures. Classical methods such as maximum likelihood remain widely used because of their desirable large-sample properties, whereas Bayesian methods have received increasing attention for incorporating prior information and quantifying parameter uncertainty in complex stochastic models. Recent developments include online Bayesian inference for identifying latent degradation states [29], bivariate Wiener degradation models with partially random scale weights [30], and hierarchical Bayesian multivariate Wiener process models for joint parameter estimation and uncertainty quantification [31]. These developments demonstrate the increasing importance of flexible inferential techniques in modern reliability and stochastic modeling.

In the present study, inference for the parameter θ of the PTS-XL distribution is considered using four classical estimation procedures: The method of moments, maximum likelihood, least squares, and weighted least squares. These methods provide complementary approaches for assessing the finite-sample and asymptotic behavior of the resulting estimators.

4.1. Method of moments estimator

Assume that $x_1, x_2, \ldots, x_n$ denote a random sample from the PTS-XL distribution. The method of moments estimator (MME) for the parameter θ is obtained by equating the sample mean, $\bar{x} = \frac{1}{n}\sum_{i=1}^{n} x_i$, to the theoretical mean of the PTS-XL

$$\bar{x} = \frac{4 + 2\theta(2+\theta)}{\theta(1+\theta)^2}.$$

Solving this equation fo θ gives the MME

$$\hat{\theta}_{MME} = \frac{-\bar{x}\,(\bar{x} + 2\Delta(\bar{x}) + 4) + (2 - \Delta(\bar{x}))\Delta(\bar{x}) - 4}{3\bar{x}\,\Delta(\bar{x})}, \tag{4.1}$$

where $\Delta(\bar{x}) = \left(-\bar{x}^3 - 33\bar{x}^2 - 12\bar{x} - 8 + 3^{3/2}\bar{x}(2\bar{x}^3 + 39\bar{x}^2 + 24\bar{x} + 16)^{1/2}\right)^{1/3}$.

4.2. Maximum likelihood estimator

Let $x_1, x_2, \ldots, x_n$ be a random sample from the PTS-XL distribution. The corresponding likelihood function is

$$L(\theta) = \prod_{i=1}^{n} P(X = x_i; \theta). \tag{4.2}$$

By substituting the PMF given in (2.9) and taking the natural logarithm, the log-likelihood function is given by

$$\begin{aligned}\ell(\theta) =&4n\log\theta - n\log 6 + \sum_{i=1}^{n}\log(1+x_i) - \sum_{i=1}^{n}(x_i+8)\log(1+\theta) \\ &+ \sum_{i=1}^{n}\log\left[x_i^2 + x_i\left(17+6\theta(\theta+3)\right) + 6\{3+\theta(\theta+3)\}^2\right].\end{aligned} \tag{4.3}$$

The maximum likelihood estimate (MLE) of θ, denoted by $\hat{\theta}_{ML}$, is obtained by solving the corresponding likelihood equation

$$\frac{\partial\ell(\theta)}{\partial\theta} = \frac{4n}{\theta} - \frac{1}{1+\theta}\sum_{i=1}^{n}(x_i+8) + 6(2\theta+3)\sum_{i=1}^{n}\frac{x_i+2\theta(\theta+3)+6}{x_i^2+x_i(17+6\theta(\theta+3))+6\{3+\theta(\theta+3)\}^2} = 0. \tag{4.4}$$

Since this equation is nonlinear in θ, the MLE $\hat{\theta}_{ML}$ must be obtained numerically. In this study, the computations are carried out using `Mathematica`, which implements methods including the Newton–Raphson algorithm through functions like `FindMaximum` and `FindRoot`.

4.3. Least squares and weighted least squares estimators

Let $x_{(1)}, x_{(2)}, \ldots, x_{(n)}$ denote the ordered sample from the PTS-XL distribution. The least squares estimator (LSE) is obtained by minimizing the squared deviations between the theoretical CDF and the corresponding empirical probabilities. Specifically, the LSE estimate of the parameter θ, denoted by $\hat{\theta}_{LS}$, is obtained by minimizing the objective function

$$LS(\theta) = \sum_{i=1}^{n}\left[F(x_{(i)};\theta) - \frac{i}{n+1}\right]^2, \tag{4.5}$$

where $F(x;\theta)$ is given by (2.11). Hence,

$$LS(\theta) = \sum_{i=1}^{n}\left[1 - \frac{1}{6}(1+\theta)^{-x_{(i)}-8}\left[\omega_0(\theta) + \omega_1(\theta)x_{(i)} + \omega_2(\theta)x_{(i)}^2 + \theta^3 x_{(i)}^3\right] - \frac{i}{n+1}\right]^2. \tag{4.6}$$

The weighted least squares estimator (WLSE) assigns different weights to the squared deviations in order to account for the unequal variability of the empirical distribution function. The WLSE estimate of θ, denoted by $\hat{\theta}_{WLS}$. The corresponding objective function is

$$WLS(\theta) = \sum_{i=1}^{n}\frac{(n+1)^2(n+2)}{i(n-i+1)}\left[F(x_{(i)};\theta) - \frac{i}{n+1}\right]^2. \tag{4.7}$$

Equivalently, we have

$$WLS(\theta) = \sum_{i=1}^{n}\frac{(n+1)^2(n+2)}{i(n-i+1)}\left[1 - \frac{1}{6}(1+\theta)^{-x_{(i)}-8}\left[\omega_0(\theta) + \omega_1(\theta)x_{(i)} + \omega_2(\theta)x_{(i)}^2 + \theta^3 x_{(i)}^3\right] - \frac{i}{n+1}\right]^2. \tag{4.8}$$

The minimization of the objective functions given in (4.6) and (4.8) does not admit closed-form solutions and therefore requires numerical optimization techniques. In this study, the estimates are obtained using `Mathematica` through built-in routines such as `FindMinimum` and `FindRoot`.

5. Interval estimation

This section discusses interval estimation for the parameter θ of the PTS-XL distribution.

5.1. Asymptotic confidence interval

Let $\hat{\theta}_{\mathrm{ML}}$ is the MLE of the parameter θ, the asymptotic confidence interval (ACI) is constructed on the basis of the well-established asymptotic normality of $\hat{\theta}_{\mathrm{ML}}$. Under standard regularity conditions, the asymptotic distribution of $(\hat{\theta}_{\mathrm{ML}} - \theta)$ is $\sqrt{n}\,(\hat{\theta}_{\mathrm{ML}} - \theta) \xrightarrow{d} \mathcal{N}(0, I^{-1}(\theta))$, where $I(\theta)$ denotes the Fisher information. In practice, the variance is approximated using the observed information evaluated at $\hat{\theta}_{\mathrm{ML}}$, defined as

$$I^{-1}(\hat{\theta}_{\mathrm{ML}}) = \left[-\frac{\partial^2 \ell(\theta)}{\partial \theta^2}\right]^{-1}_{\theta=\hat{\theta}_{\mathrm{ML}}}, \tag{5.1}$$

where

$$\begin{aligned}\frac{\partial^2 \ell(\theta)}{\partial \theta^2} &= -\frac{4n}{\theta^2} + \frac{1}{(1+\theta)^2}\sum_{i=1}^{n}(x_i+8) \\ &+ 12\sum_{i=1}^{n}\frac{x_i^3 + 5x_i^2 - 3x_i\Big(5 + 2\theta(\theta+3)(4+\theta(\theta+3))\Big) - 6(3+\theta(\theta+3))^2(3+2\theta(\theta+3))}{\left[x_i^2 + x_i(17 + 6\theta(\theta+3)) + 6(3+\theta(\theta+3))^2\right]^2}.\end{aligned}$$

Therefore, for $\alpha \in (0,1)$, the $100(1-\alpha)\%$ ACI for θ is $\hat{\theta}_{\mathrm{ML}} \pm z_{\alpha/2}\sqrt{I^{-1}(\hat{\theta}_{\mathrm{ML}})}$, where $z_{\alpha/2}$ denotes the upper $\alpha/2$ standard normal quantile.

5.2. Bootstrap confidence intervals

The ACI for θ is constructed on the basis of the normal approximation of the MLE. The finite-sample performance of this approach may not be sufficiently accurate, particularly for small sample sizes. To address this limitation, bootstrap confidence intervals are commonly used as alternative procedures that often provide improved performance in small samples. The two type of bootstrap intervals are the percentile bootstrap (Boot-p) and the standardized bootstrap (Boot-t) confidence intervals [32].

5.2.1. Boot-p intervals

Boot-p intervals use the empirical distribution of the parameter estimates obtained from repeated bootstrap samples. The confidence interval is then based on the percentile of this empirical distribution. The following steps describe the construction of the Boot-p interval of θ.

(1) Obtain the MLE $\hat{\theta}_{\mathrm{ML}}$ using the observed sample.
(2) Generate the bootstrap sample from the PTS-XL distribution with the parameter $\hat{\theta}_{\mathrm{ML}}$.
(3) Obtain the bootstrap estimate $\hat{\theta}^*$ of θ under the bootstrap sample.
(4) Repeat Steps (2) and (3) B times to obtain $\hat{\theta}^*_1, \hat{\theta}^*_2, \ldots, \hat{\theta}^*_B$.
(5) Form the ordered bootstrap estimates, $\hat{\theta}^*_{(1)} < \hat{\theta}^*_{(2)} < \ldots, \hat{\theta}^*_{(B)}$, for some value $\alpha, (0 < \alpha < 1)$, the $100(1-\alpha)\%$ Boot-p interval for the parameter θ is given by $\left[\hat{\theta}^*_{[B\alpha/2]},\ \hat{\theta}^*_{[B(1-\alpha/2)]}\right]$, where $[c]$ denotes the integer part of c.

5.2.2. Boot-t intervals

The Boot-t interval uses the empirical distribution of the standardized statistics obtained from repeated bootstrap samples. The confidence interval is then based on the percentiles of this empirical distribution. The following steps describe the construction of the Boot-t interval of θ.

(1) Repeat Steps (1) to (4) of the Boot-p steps to generate B bootstrap estimates $\hat{\theta}^*_1, \hat{\theta}^*_2, \ldots, \hat{\theta}^*_B$.
(2) Obtain the standardized statistic $\hat{T}^*$ for each bootstrap estimate as

$$\hat{T}^*_l = \frac{\hat{\theta}^*_l - \hat{\theta}_{ML}}{\sqrt{I^{-1}(\hat{\theta}^*_l)}}, \quad l = 1, \ldots, B.$$

(3) Sort the resulting statistics in ascending order to get $\hat{T}^*_{(1)} < \hat{T}^*_{(2)}, \ldots, \hat{T}^*_{(B)}$.
(4) For a given significance level α $(0 < \alpha < 1)$, the $100(1-\alpha)\%$ Boot-t confidence interval for θ is

$$\left[\hat{\theta}_{\mathrm{ML}} + \hat{T}^*_{([B\alpha/2])} \cdot \sqrt{I^{-1}(\hat{\theta}_{\mathrm{ML}})},\ \hat{\theta}_{\mathrm{ML}} + \hat{T}^*_{([B(1-\alpha/2)])} \cdot \sqrt{I^{-1}(\hat{\theta}_{\mathrm{ML}})}\right].$$

6. Simulation

This section conducts a comprehensive Monte Carlo simulation study to assess the performance of the estimators of the parameter θ. Samples of sizes $n = 25, 50, 75, 100, 200, 400$, and 600 are generated from the proposed PTS-XL distribution. Different true values for the parameter, $\theta_0 = 0.1, 0.5, 1.1, 1.5$, and 2.2, were selected to examine the behavior of the estimators under different distributional shapes and dispersion levels. For each combination of the n and θ_0, $N = 5000$ independent samples were generated. The MLE, LSE, and WLSE are obtained numerically using Mathematica version 14 through numerical routines such as `FindRoot`, `FindMaximum`, and `FindMinimum`. The numerical procedures showed satisfactory convergence across the considered simulation scenarios, with only a negligible number of unsuccessful optimization attempts, which were restarted until convergence was achieved. The computational time required for numerical estimation was generally less than 0.015 seconds per run, indicating a low computational cost. Sensitivity to the choice of starting values was also examined, and the numerical procedures converged to essentially the same estimates across the considered initial values, indicating satisfactory numerical stability.

The performance of the point estimators is evaluated by using mean squared error (MSE), average absolute bias (AAB), and mean relative error (MRE). Furthermore, the 95% ACI, Boot-p, and Boot-t intervals are obtained for θ, where $B = 1000$ bootstrap samples are used to construct the Boot-p and Boot-t intervals. The interval estimators are evaluated using the average length (AL) and coverage probability (CP). These performance measures are summarized in Table 3.

Table 3. Summary of the performance measures used in the simulation study.

Assessment	Measure	Definition	Description
Point estimation	MSE	$\frac{1}{N}\sum_{i=1}^{N}(\hat{\theta}_i-\theta_0)^2$	Average squared estimation error.
	AAB	$\frac{1}{N}\sum_{i=1}^{N}\lvert\hat{\theta}_i-\theta_0\rvert$	Average absolute deviation from the true value.
	MRE	$\frac{1}{N}\sum_{i=1}^{N}\left\lvert\frac{\hat{\theta}_i-\theta_0}{\theta_0}\right\rvert$	Average error relative to the true value.
Interval estimation	AL	$\frac{1}{N}\sum_{i=1}^{N}(U_i-L_i)$	Average width of the confidence intervals.
	CP	$\frac{1}{N}\sum_{i=1}^{N}I(L_i\leq\theta_0\leq U_i)$	Proportion of intervals containing the true value.

Here, L_i and U_i denote the lower and upper bounds of the confidence interval in the i-th replication, respectively, and $I(\cdot)$ refers to the indicator function. The simulation results are reported in Tables 4–9 and graphically summarized through the heat maps in Figures 4 and 5 for the point and interval estimation results, respectively. The following observations can be made.

- All point estimators exhibit satisfactory performance, with decreasing values of MSE, AAB, and MRE as the sample size increases.
- The MLE and MME exhibit very similar performance, with a marginal advantage for the MLE. Both methods generally provide the best performance, with the smallest MSE, AAB, and MRE, especially for small and moderate values of θ.
- The LSE and WLSE demonstrate a weaker performance compared with the MLE and MME for small and moderate values of θ_0.
- For larger values of θ_0, the performance of the estimators changes. At $\theta_0 = 2.2$, the LSE provides the smallest MSE, AAB, and MRE for small and moderate sample sizes, while the MLE and MME become more competitive as the sample size increases.
- Overall, the MLE emerges as the most reliable and efficient method across different settings, followed by the MME. The WLSE offers a reasonable compromise, while the LSE appears less competitive.
- For the interval estimators, the AL decreases as the sample size increases for the ACI, Boot-p, and Boot-t methods, while the CPs remain reasonably close to the nominal level of 95% in most scenarios.
- The ACI, Boot-p, and Boot-t intervals show comparable performance for small and moderate values of θ_0. For larger values of θ_0 and small sample sizes, however, the Boot-t intervals tend to show lower CPs, while the Boot-p and ACI intervals remain closer to the nominal level. This difference becomes less pronounced as the sample size increases.
- Larger values of θ_0 lead to wider confidence intervals, reflecting the higher uncertainty in our estimates.

Overall, the simulation study shows that all point estimation methods become more accurate as the sample size increases. The MLE and MME provide competitive performance for small and moderate values of θ_0, while the LSE becomes particularly competitive for larger parameter values. For interval estimation, the ACI, Boot-p, and Boot-t intervals become narrower as the sample size increases, with coverage probabilities generally close to the nominal 95% level.

Table 4. Simulation analysis for estimators of θ with the PTS-XL distribution and the true value $\theta_0 = 0.1$.

Estimation method	Criterion	25	50	75	100	200	400	600
MLE	MSE	0.00013	0.00006	0.00004	0.00003	0.00001	6.668×10^{-6}	4.374×10^{-6}
	MRE	0.08916	0.05875	0.05035	0.04486	0.03026	0.02046	0.01672
	AAB	0.00892	0.00587	0.00504	0.00449	0.00303	0.00205	0.00167
MME	MSE	0.00013	0.00006	0.00004	0.00003	0.00001	7.072×10^{-6}	4.516×10^{-6}
	MRE	0.09049	0.06289	0.05150	0.04582	0.02926	0.02110	0.01737
	AAB	0.00905	0.00629	0.00515	0.00458	0.00293	0.00211	0.00174
LSE	MSE	0.00015	0.00007	0.00005	0.00004	0.00002	6.823×10^{-6}	4.829×10^{-6}
	MRE	0.09759	0.06956	0.05760	0.04603	0.03364	0.01998	0.01777
	AAB	0.00976	0.00696	0.00576	0.00460	0.00336	0.00200	0.00178
WLSE	MSE	0.00015	0.00007	0.00005	0.00003	0.00002	6.273×10^{-6}	4.474×10^{-6}
	MRE	0.09493	0.06733	0.05532	0.04489	0.03259	0.01909	0.01709
	AAB	0.00949	0.00673	0.00553	0.00449	0.00326	0.00191	0.00171

Table 5. Simulation analysis for estimators of θ with the PTS-XL distribution and the true value $\theta_0 = 0.5$.

Estimation method	Criterion	25	50	75	100	200	400	600
MLE	MSE	0.00396	0.00214	0.00140	0.00102	0.00052	0.00027	0.00014
	MRE	0.09879	0.07274	0.05864	0.05045	0.03681	0.02667	0.01880
	AAB	0.04939	0.03637	0.02932	0.02522	0.01841	0.01334	0.00940
MME	MSE	0.00480	0.00208	0.00150	0.00112	0.00053	0.00024	0.00016
	MRE	0.10870	0.07110	0.06145	0.05381	0.03649	0.02460	0.02014
	AAB	0.05435	0.03555	0.03073	0.02691	0.01825	0.01230	0.01007
LSE	MSE	0.00788	0.00292	0.00226	0.00159	0.00100	0.00051	0.00042
	MRE	0.13250	0.08676	0.07612	0.06410	0.04981	0.03519	0.03141
	AAB	0.06625	0.04338	0.03806	0.03205	0.02490	0.01760	0.01570
WLSE	MSE	0.00738	0.00267	0.00202	0.00141	0.00088	0.00043	0.00034
	MRE	0.12839	0.08348	0.07184	0.06034	0.04666	0.03186	0.02804
	AAB	0.06419	0.04174	0.03592	0.03017	0.02333	0.01593	0.01402

Table 6. Simulation analysis for estimators of θ with the PTS-XL distribution and the true value $\theta_0 = 1.1$.

Estimation method	Criterion	25	50	75	100	200	400	600
MLE	MSE	0.04334	0.01820	0.01201	0.00877	0.00417	0.00190	0.00125
	MRE	0.14463	0.09327	0.07814	0.06792	0.04635	0.03095	0.02576
	AAB	0.15909	0.10260	0.08596	0.07472	0.05099	0.03405	0.02834
MME	MSE	0.04339	0.01818	0.01201	0.00878	0.00417	0.00190	0.00125
	MRE	0.14460	0.09324	0.07815	0.06793	0.04638	0.03091	0.02575
	AAB	0.15906	0.10257	0.08596	0.07472	0.05101	0.03400	0.02832
LSE	MSE	0.07101	0.03271	0.02262	0.01495	0.00959	0.00636	0.00618
	MRE	0.18309	0.12069	0.10361	0.08794	0.07209	0.05797	0.05911
	AAB	0.20140	0.13276	0.11397	0.09674	0.07930	0.06377	0.06503
WLSE	MSE	0.06213	0.02708	0.01766	0.01097	0.00659	0.00384	0.00350
	MRE	0.17130	0.11127	0.09185	0.07547	0.05928	0.04392	0.04262
	AAB	0.18843	0.12240	0.10103	0.08302	0.06521	0.04831	0.04688

Table 7. Simulation analysis for estimators of θ with the PTS-XL distribution and the true value $\theta_0 = 1.5$.

Estimation method	Criterion	25	50	75	100	200	400	600
MLE	MSE	0.11821	0.04484	0.02969	0.02186	0.00983	0.00473	0.00300
	MRE	0.16918	0.10732	0.08956	0.07765	0.05196	0.03588	0.02914
	AAB	0.25377	0.16097	0.13433	0.11648	0.07795	0.05382	0.04371
MME	MSE	0.11824	0.04481	0.02969	0.02187	0.00985	0.00474	0.00300
	MRE	0.16916	0.10731	0.08949	0.07764	0.05198	0.03589	0.02913
	AAB	0.25375	0.16096	0.13424	0.11646	0.07797	0.05384	0.04369
LSE	MSE	0.09939	0.05016	0.03278	0.02551	0.01720	0.00954	0.00861
	MRE	0.16474	0.12210	0.09576	0.08546	0.06916	0.05127	0.05014
	AAB	0.24711	0.18315	0.14364	0.12819	0.10374	0.07691	0.07521
WLSE	MSE	0.09394	0.04406	0.02750	0.02012	0.01226	0.00563	0.00445
	MRE	0.15865	0.11476	0.08802	0.07471	0.05855	0.03900	0.03523
	AAB	0.23798	0.17215	0.13203	0.11206	0.08782	0.05850	0.05285

Table 8. Simulation analysis for estimators of θ with the PTS-XL distribution and the true value $\theta_0 = 2.2$.

Estimation method	Criterion	25	50	75	100	200	400	600
MLE	MSE	0.35700	0.13918	0.09774	0.06994	0.02634	0.01394	0.00992
	MRE	0.20053	0.12953	0.10925	0.09339	0.05853	0.04236	0.03613
	AAB	0.44117	0.28496	0.24036	0.20545	0.12876	0.09320	0.07948
MME	MSE	0.40212	0.13855	0.09922	0.06896	0.03005	0.01517	0.00912
	MRE	0.20844	0.12897	0.11021	0.09263	0.06256	0.04352	0.03481
	AAB	0.45856	0.28374	0.24246	0.20379	0.13764	0.09575	0.07659
LSE	MSE	0.13817	0.06727	0.05169	0.03388	0.02123	0.01544	0.01416
	MRE	0.13637	0.09610	0.08392	0.06853	0.05304	0.04717	0.04565
	AAB	0.30000	0.21143	0.18463	0.15077	0.11669	0.10378	0.10044
WLSE	MSE	0.16139	0.08022	0.06298	0.04393	0.02896	0.02268	0.02164
	MRE	0.14780	0.10547	0.09391	0.07884	0.06264	0.05872	0.05838
	AAB	0.32516	0.23203	0.20660	0.17344	0.13781	0.12919	0.12843

Table 9. AL and CP of the 95% confidence intervals for θ.

Parameter	Method	Criterion	25	50	75	100	200	400	600
$\theta_0 = 0.1$	ACI	AL	0.04225	0.02939	0.02397	0.02062	0.01456	0.01034	0.00840
		CP	0.943	0.950	0.943	0.945	0.938	0.953	0.955
	Boot-p	AL	0.04343	0.03010	0.02389	0.02091	0.01483	0.01046	0.00852
		CP	0.932	0.972	0.944	0.944	0.964	0.952	0.964
	Boot-t	AL	0.04207	0.02966	0.02367	0.02078	0.01479	0.01043	0.00851
		CP	0.952	0.956	0.932	0.944	0.964	0.964	0.960
$\theta_0 = 0.5$	ACI	AL	0.25363	0.17682	0.1434	0.12487	0.08763	0.06229	0.05056
		CP	0.956	0.952	0.954	0.948	0.960	0.951	0.948
	Boot-p	AL	0.26692	0.18153	0.14518	0.12763	0.08928	0.06299	0.05124
		CP	0.960	0.940	0.948	0.952	0.956	0.932	0.948
	Boot-t	AL	0.24824	0.17520	0.14288	0.12556	0.08865	0.06280	0.05112
		CP	0.940	0.928	0.924	0.948	0.944	0.940	0.960
$\theta_0 = 1.1$	ACI	AL	0.75361	0.50682	0.40966	0.34951	0.24526	0.17467	0.14101
		CP	0.938	0.953	0.945	0.948	0.943	0.958	0.945
	Boot-p	AL	0.81008	0.52690	0.42250	0.36267	0.25228	0.17506	0.14262
		CP	0.944	0.928	0.936	0.936	0.948	0.980	0.960
	Boot-t	AL	0.68564	0.48757	0.40251	0.35100	0.24754	0.17362	0.14180
		CP	0.916	0.924	0.920	0.932	0.928	0.960	0.960
$\theta_0 = 1.5$	ACI	AL	1.20980	0.79748	0.64066	0.54557	0.38145	0.27180	0.21891
		CP	0.943	0.960	0.945	0.938	0.935	0.958	0.963
	Boot-p	AL	1.25720	0.85886	0.65379	0.56886	0.39590	0.27222	0.22320
		CP	0.964	0.924	0.952	0.960	0.948	0.968	0.932
	Boot-t	AL	1.09619	0.77676	0.62131	0.54212	0.38738	0.26901	0.22175
		CP	0.917	0.932	0.932	0.960	0.948	0.956	0.952
$\theta_0 = 2.2$	ACI	AL	2.22232	1.42772	1.14081	0.96252	0.67050	0.47894	0.38403
		CP	0.960	0.965	0.948	0.938	0.955	0.965	0.945
	Boot-p	AL	2.03341	1.53753	1.18476	1.01974	0.69319	0.48418	0.39175
		CP	0.964	0.904	0.960	0.952	0.968	0.932	0.924
	Boot-t	AL	1.81140	1.34550	1.08730	0.95507	0.67288	0.47549	0.38790
		CP	0.897	0.912	0.912	0.932	0.956	0.932	0.936

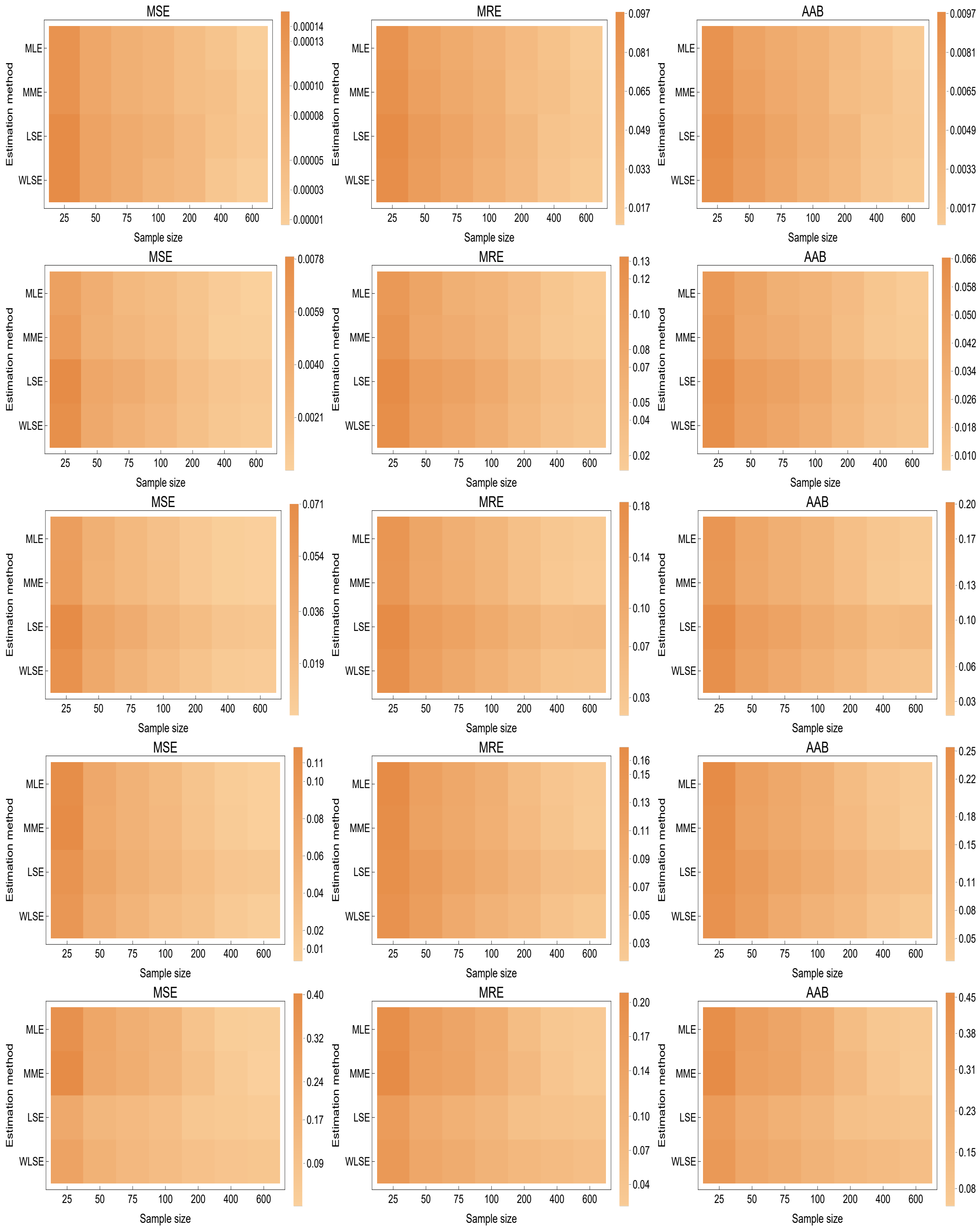

Figure 4. Heat maps of the MSE, MRE, and AAB for the PTS-XL estimators. From top to bottom, the rows correspond to $\theta_0 = 0.1,\ 0.5,\ 1.1,\ 1.5$, and 2.2, respectively.

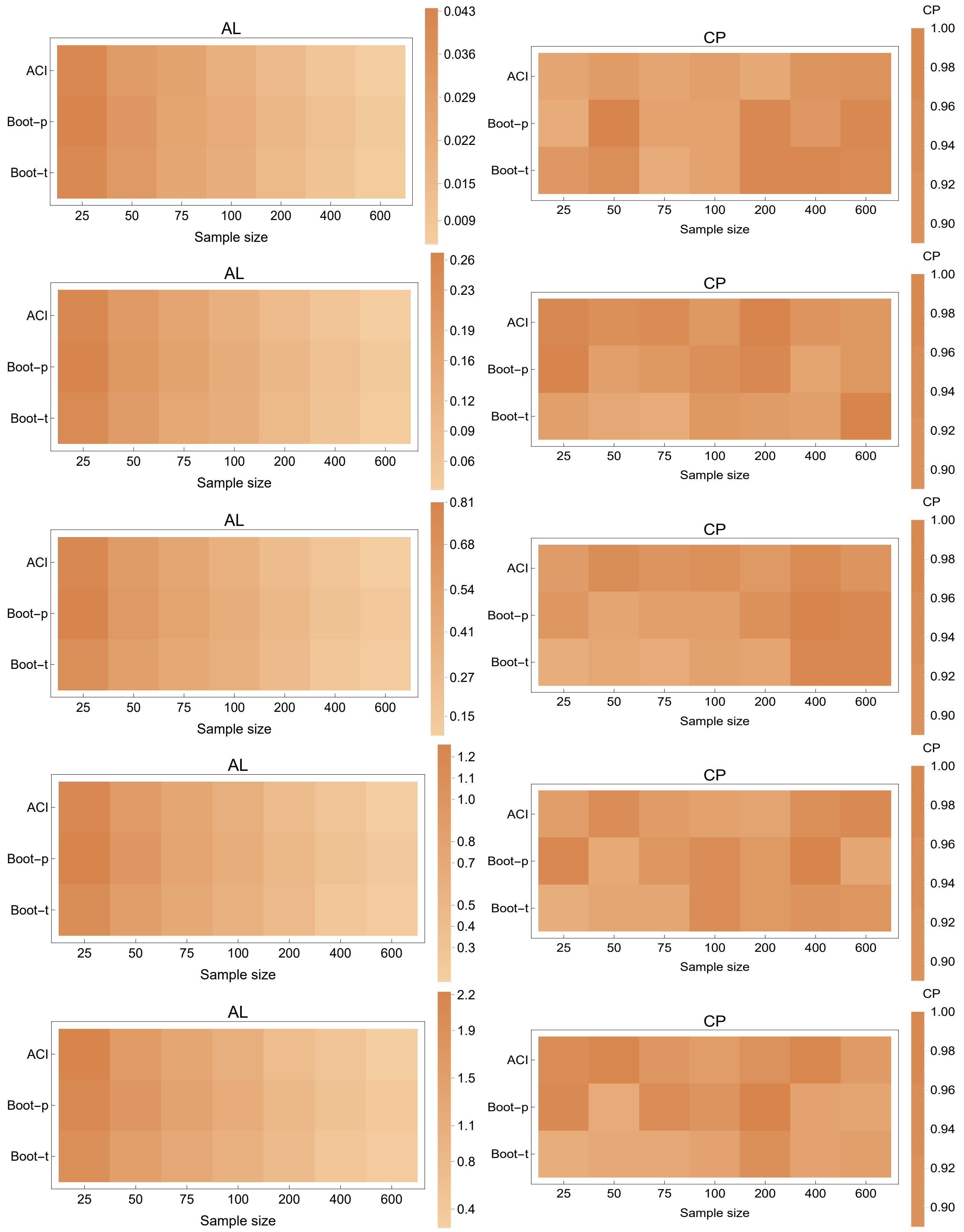

Figure 5. Heat maps of the AL and CP for the 95% confidence intervals of θ. From top to bottom, the rows correspond to $\theta_0 = 0.1,\ 0.5,\ 1.1,\ 1.5$, and 2.2, respectively.

7. PTS-XL regression model

Count regression models are essential for modeling discrete response data affected by covariate information. However, the Poisson regression model is commonly adopted for such data, and its equidispersion assumption is often violated in practice. Therefore, this section proposes a count regression model based on the PTS-XL distribution to provide greater flexibility modeling overdispersed count responses.

7.1. Model description

Let Y_i be a count response variable for the ith observation, $i = 1, \ldots, n$, following the PTS-XL distribution with the parameter θ_i, and satisfy

$$E(Y_i) = \mu_i = \frac{4 + 2\theta_i(2 + \theta_i)}{\theta_i(1 + \theta_i)^2}.$$

Apply the parameterization

$$\theta_i = \frac{-\mu_i\,(\mu_i + 2\Delta_i + 4) + (2 - \Delta_i)\Delta_i - 4}{3\mu_i\,\Delta_i}, \tag{7.1}$$

where

$$\Delta_i = \left(-\mu_i^3 - 33\mu_i^2 - 12\mu_i - 8 + 3\sqrt{3}\mu_i\sqrt{2\mu_i^3 + 39\mu_i^2 + 24\mu_i + 16}\right)^{1/3}. \tag{7.2}$$

To incorporate the effect of the covariates, μ_i corresponds to the covariates via the log-link function

$$\mu_i = \exp(\mathbf{x}_i^\top \boldsymbol{\beta}), i = 1, \ldots, n, \tag{7.3}$$

where $\mathbf{x}_i = (1, x_{i1}, x_{i2}, \ldots, x_{ip})^\top$ denotes the covariate vector that has a full column rank, and $\boldsymbol{\beta} = (\beta_0, \beta_1, \ldots, \beta_p)^\top$ denotes the vector of regression coefficients. Accordingly, $Y_i \mid \mathbf{x}_i \sim$ PTS-XL(θ_i), where $\theta_i = \theta(\mu_i)$. Thus, μ_i serves as a mean-based reparameterization of the original PTS-XL parameter θ_i.

$$\begin{aligned} P(Y_i = y_i \mid \mathbf{x}_i) = {} & \frac{1}{6}(1 + y_i)\left[\frac{-\mu_i\,(\mu_i + 2\Delta_i + 4) + (2 - \Delta_i)\Delta_i - 4}{3\mu_i\Delta_i}\right]^4 \\ & \times\left(1 + \left[\frac{-\mu_i\,(\mu_i + 2\Delta_i + 4) + (2 - \Delta_i)\Delta_i - 4}{3\mu_i\Delta_i}\right]\right)^{-(y_i+8)} \\ & \times\Bigg\{y_i^2 + y_i\Bigg[17 + 6\left(\frac{-\mu_i\,(\mu_i + 2\Delta_i + 4) + (2 - \Delta_i)\Delta_i - 4}{3\mu_i\Delta_i}\right) \\ & \qquad \times\left(\frac{-\mu_i\,(\mu_i + 2\Delta_i + 4) + (2 - \Delta_i)\Delta_i - 4}{3\mu_i\Delta_i} + 3\right)\Bigg] \\ & + 6\Bigg[3 + \left(\frac{-\mu_i\,(\mu_i + 2\Delta_i + 4) + (2 - \Delta_i)\Delta_i - 4}{3\mu_i\Delta_i}\right) \\ & \qquad \times\left(\frac{-\mu_i\,(\mu_i + 2\Delta_i + 4) + (2 - \Delta_i)\Delta_i - 4}{3\mu_i\Delta_i} + 3\right)\Bigg]^2\Bigg\}, \end{aligned} \tag{7.4}$$

where Δ_i is given by (7.2), with μ_i defined in (7.3).

7.2. *Identifiability and inferential properties*

Before discussing parameter estimation, we establish some theoretical properties of the proposed PTS-XL regression model.

Proposition 1. *The mapping $\theta \mapsto \mu(\theta)$ is one-to-one from $(0, \infty)$ onto $(0, \infty)$. Consequently, the mean parameterization of the PTS-XL distribution is identifiable.*

Proof. Differentiating $\mu(\theta)$ with respect to θ gives

$$\frac{d\mu(\theta)}{d\theta} = -\frac{2(\theta^3 + 3\theta^2 + 6\theta + 2)}{\theta^2(1 + \theta)^3}.$$

For every $\theta > 0$, both the denominator and the polynomial in the numerator are positive. Hence,

$$\frac{d\mu(\theta)}{d\theta} < 0,$$

so $\mu(\theta)$ is strictly decreasing.

Furthermore,

$$\lim_{\theta\to 0^+} \mu(\theta) = \infty, \qquad \lim_{\theta\to\infty} \mu(\theta) = 0.$$

Thus, $\mu(\theta)$ defines a continuous one-to-one mapping from $(0, \infty)$ onto $(0, \infty)$ and consequently admits a unique inverse $\theta = \theta(\mu)$. □

Using the log-link function (7.3), suppose that two parameter vectors $\boldsymbol{\beta}_1$ and $\boldsymbol{\beta}_2$ generate the same conditional distributions for all observations. Since the PTS-XL family is identifiable through its mean parameter,

$$\exp(\mathbf{x}_i^\top \boldsymbol{\beta}_1) = \exp(\mathbf{x}_i^\top \boldsymbol{\beta}_2)$$

for every i. The exponential function is one-to-one, and hence $\mathbf{X}(\boldsymbol{\beta}_1 - \boldsymbol{\beta}_2) = \mathbf{0}$. Since $\mathbf{X}$ has a full column rank, $\boldsymbol{\beta}_1 = \boldsymbol{\beta}_2$. Therefore, the PTS-XL regression model is identifiable.

7.3. *Parameter estimation*

This subsection uses the maximum likelihood method to estimate the regression parameter vector $\boldsymbol{\beta} = (\beta_0, \beta_1, \ldots, \beta_p)^\top$. The log-likelihood function for the PTS-XL count regression model is

$$
\begin{aligned}
\ell(\boldsymbol{\beta}) = n\log\left(\frac{1}{6}\right) &+ \sum_{i=1}^{n}\log(1+y_i)\\
&+ 4\sum_{i=1}^{n}\log\left(\frac{-\mu_i\,(\mu_i+2\Delta_i+4)+(2-\Delta_i)\Delta_i-4}{3\mu_i\Delta_i}\right)\\
&- \sum_{i=1}^{n}(y_i+8)\log\left[1+\frac{-\mu_i\,(\mu_i+2\Delta_i+4)+(2-\Delta_i)\Delta_i-4}{3\mu_i\Delta_i}\right]\\
&+ \sum_{i=1}^{n}\log\left\{y_i^2+y_i\left[17+6\left(\frac{-\mu_i\,(\mu_i+2\Delta_i+4)+(2-\Delta_i)\Delta_i-4}{3\mu_i\Delta_i}\right)\right.\right.\\
&\qquad\qquad\left.\times\left(\frac{-\mu_i\,(\mu_i+2\Delta_i+4)+(2-\Delta_i)\Delta_i-4}{3\mu_i\Delta_i}+3\right)\right]\\
&\quad+6\left[3+\left(\frac{-\mu_i\,(\mu_i+2\Delta_i+4)+(2-\Delta_i)\Delta_i-4}{3\mu_i\Delta_i}\right)\right.\\
&\qquad\qquad\left.\left.\times\left(\frac{-\mu_i\,(\mu_i+2\Delta_i+4)+(2-\Delta_i)\Delta_i-4}{3\mu_i\Delta_i}+3\right)\right]^2\right\}.
\end{aligned}
\tag{7.5}
$$

The score vector for the regression parameter $\boldsymbol{\beta}$ is defined by

$$\mathbf{U}(\boldsymbol{\beta}) = \frac{\partial\ell(\boldsymbol{\beta})}{\partial\boldsymbol{\beta}} = \sum_{i=1}^{n}\frac{\partial\ell_i}{\partial\theta_i}\frac{d\theta_i}{d\mu_i}\frac{d\mu_i}{d\eta_i}\frac{\partial\eta_i}{\partial\boldsymbol{\beta}},$$

where $\eta_i = \mathbf{x}_i^\top\boldsymbol{\beta}$ and $\mu_i = \exp(\eta_i)$. Therefore, we have

$$\frac{d\mu_i}{d\eta_i} = \mu_i, \qquad \frac{\partial\eta_i}{\partial\boldsymbol{\beta}} = \mathbf{x}_i.$$

Furthermore, since

$$\mu_i = \frac{4+2\theta_i(2+\theta_i)}{\theta_i(1+\theta_i)^2},$$

differentiation with respect to θ_i gives

$$\frac{d\mu_i}{d\theta_i} = -\frac{2(\theta_i^3+3\theta_i^2+6\theta_i+2)}{\theta_i^2(1+\theta_i)^3}.$$

Since this derivative is nonzero for every $\theta_i > 0$, the inverse function theorem gives

$$\frac{d\theta_i}{d\mu_i} = -\frac{\theta_i^2(1+\theta_i)^3}{2(\theta_i^3+3\theta_i^2+6\theta_i+2)}.$$

Consequently, the score vector can be expressed as

$$\mathbf{U}(\boldsymbol{\beta}) = \sum_{i=1}^{n}\left(\frac{\partial\ell_i}{\partial\theta_i}\right)\left[-\frac{\theta_i^2(1+\theta_i)^3}{2(\theta_i^3+3\theta_i^2+6\theta_i+2)}\right]\mu_i\,\mathbf{x}_i.$$

The MLE $\widehat{\boldsymbol{\beta}}$ is obtained by solving $\mathbf{U}(\widehat{\boldsymbol{\beta}}) = \mathbf{0}$ or, equivalently, by directly maximizing $\ell(\boldsymbol{\beta})$. Since these equations do not admit a closed-form solution, numerical optimization is required. In this study, we used the functions FindRoot and FindMaximum in Mathematica software version 14.

7.3.1. Existence, uniqueness, and asymptotic property of the MLE

Let $\Omega \subset \mathbb{R}^{p+1}$ denote the parameter space of $\boldsymbol{\beta}$, where p is the number of unknown parameters. For a finite sample, the log-likelihood $\ell(\boldsymbol{\beta})$ is continuous in $\boldsymbol{\beta}$ because $\mu_i = \exp(\mathbf{x}_i^\top \boldsymbol{\beta}) > 0$ and the inverse mapping $\theta(\mu_i)$ is continuous. Since the log-likelihood function $\ell(\boldsymbol{\beta})$ is continuous in $\boldsymbol{\beta}$, the Weierstrass extreme value theorem guarantees that $\ell(\boldsymbol{\beta})$ reaches its maximum on any nonempty compact parameter space $\Omega \subset \mathbb{R}^{p+1}$; see, for example, Rudin [33].

Because the log-likelihood is nonlinear and global strict concavity has not been established, finite-sample global uniqueness is not claimed. In practice, numerical optimization is performed from various starting values to evaluate the stability of the obtained maximum.

Theorem 7.1. *Let $\boldsymbol{\beta}_0$ denote the true regression parameter. Assume the following:*

1. *$Y_1, \ldots, Y_n$ are independent conditional on the covariates;*
2. *$\boldsymbol{\beta}_0$ is an interior point of the parameter space;*
3. *the design matrix has a full column rank and the covariates are uniformly bounded;*
4. *the log-likelihood is twice continuously differentiable in a neighborhood of $\boldsymbol{\beta}_0$;*
5. *the normalized Fisher information matrix*

$$\mathbf{J}_n(\boldsymbol{\beta}_0) = -\frac{1}{n} E\left[\frac{\partial^2 \ell(\boldsymbol{\beta})}{\partial \boldsymbol{\beta} \partial \boldsymbol{\beta}^\top}\right]_{\boldsymbol{\beta}=\boldsymbol{\beta}_0}$$

converges to a finite positive-definite matrix $\mathbf{J}(\boldsymbol{\beta}_0)$.

Then the MLE is consistent,

$$\widehat{\boldsymbol{\beta}} \xrightarrow{p} \boldsymbol{\beta}_0$$

and

$$\sqrt{n}\left(\widehat{\boldsymbol{\beta}} - \boldsymbol{\beta}_0\right) \xrightarrow{d} N_{p+1}\left(\mathbf{0}, \mathbf{J}(\boldsymbol{\beta}_0)^{-1}\right).$$

Moreover, the likelihood maximizer in a neighborhood of $\boldsymbol{\beta}_0$ is unique with a probability tending to one.

Proof. The strict monotonicity of $\mu(\theta)$ together with the full-rank condition on the design matrix establishes the identifiability of $\boldsymbol{\beta}$. The PTS-XL probability mass function is positive and smooth for $\theta > 0$, and the transformations $\boldsymbol{\beta} \mapsto \mu_i = \exp(\mathbf{x}_i^\top \boldsymbol{\beta})$ and $\mu_i \mapsto \theta_i$ are continuously differentiable. Therefore, under the stated regularity conditions, the result follows from the standard maximum likelihood theory for independent parametric observations. □

Consequently, under the stated regularity conditions, an MLE exists, the consistent local maximizer is asymptotically unique, and the estimator is consistent and asymptotically normal. For asymptotic inference, define the observed information matrix as

$$\mathbf{J}_n(\boldsymbol{\beta}) = -\frac{\partial^2 \ell(\boldsymbol{\beta})}{\partial \boldsymbol{\beta} \partial \boldsymbol{\beta}^\top}.$$

Under the regularity conditions stated in the preceding Theorem, the MLE is asymptotically normal.

In practice, the asymptotic covariance matrix of $\widehat{\boldsymbol{\beta}}$ is estimated using the inverse observed information matrix evaluated at the MLE

$$\widehat{\operatorname{Cov}}\left(\widehat{\boldsymbol{\beta}}\right) = \left[\mathbf{J}_n\left(\widehat{\boldsymbol{\beta}}\right)\right]^{-1} = \left[-\frac{\partial^2 \ell(\boldsymbol{\beta})}{\partial \boldsymbol{\beta} \partial \boldsymbol{\beta}^\top}\right]^{-1}_{\boldsymbol{\beta}=\widehat{\boldsymbol{\beta}}}.$$

Accordingly, the estimated standard error of $\widehat{\beta}_j$ is

$$\mathrm{SE}\left(\widehat{\beta}_j\right) = \sqrt{\left[\widehat{\mathrm{Cov}}\left(\widehat{\boldsymbol{\beta}}\right)\right]_{jj}}, \qquad j = 0, 1, \ldots, p.$$

Approximate $100(1-\alpha)\%$ confidence intervals for the regression coefficients are consequently given by

$$\widehat{\beta}_j \pm z_{\alpha/2}\,\mathrm{SE}\left(\widehat{\beta}_j\right), \qquad j = 0, 1, \ldots, p,$$

where $z_{\alpha/2}$ denotes the upper $\alpha/2$ quantile of the standard normal distribution.

7.4. Residual analysis

To assess the sufficiency of the fitted PTS-XL regression model, randomized quantile residuals (RQRs), also known as Dunn–Smyth residuals [34], are used. Let $F(y_i \mid \mathbf{x}_i)$ denote the fitted CDF of the proposed PTS-XL regression model for the ith observation. Then, for each observed count y_i, a random variable u_i is generated from the uniform distribution over the interval as follows

$$u_i \sim \mathrm{Uniform}\left(F(y_i - 1 \mid \mathbf{x}_i), F(y_i \mid \mathbf{x}_i)\right), \quad i = 1, \ldots, n. \tag{7.6}$$

The randomized quantile residual is defined as

$$r_i = \Phi^{-1}(u_i), \quad i = 1, \ldots, n, \tag{7.7}$$

where $\Phi^{-1}(\cdot)$ denotes the inverse CDF of the standard normal distribution. When the model provides an adequate fit to the given data, the RQRs are expected to approximately follow the standard normal distribution. Consequently, the adequacy of the model is assessed using two graphical diagnostic tools: A normal quantile–quantile (Q–Q) plot and a scatter plot of the RQRs against the fitted mean values. A satisfactory fit is indicated when the Q–Q plot points lie near the reference line and the residuals versus fitted values plot shows a random scatter around zero without any systematic pattern.

In addition, Pearson and deviance residuals are considered. The Pearson residual is defined as $r_i^{(P)} = (y_i - \widehat{\mu}_i)/\sqrt{\widehat{V}_i}$, where $\widehat{\mu}_i$ and $\widehat{V}_i$ denote the fitted conditional mean and variance, respectively. The deviance residual is defined as $r_i^{(D)} = \mathrm{sign}(y_i - \widehat{\mu}_i)\sqrt{d_i}$, where $d_i = 2[\ell_i(\widetilde{\theta}_i; y_i) - \ell_i(\widehat{\theta}_i; y_i)]$, with $\widetilde{\theta}_i$ denoting the parameter value that maximizes the individual log-likelihood contribution for the ith observation. Both residuals are plotted against the fitted means to detect systematic departures from the fitted model. Leverage diagnostics are also used to identify observations with potentially strong influence. Further details on the residual and influence diagnostics can be found in [35].

7.5. Simulation

A Monte Carlo simulation analysis was performed to investigate the asymptotic behavior of the MLEs for the PTS-XL regression model. The performance of the point estimators was assessed using the MSE, AAB, and MRE, whereas the interval estimators were evaluated with the AL and CP of the nominal 95% confidence intervals.

Four different regression settings are considered in the simulation. The first two involve a single covariate as follows:

$$\log(\mu_i) = \beta_0 + \beta_1 x_{i1}, \qquad i = 1, \ldots, n,$$

where the true parameter vectors (β_0, β_1) are $(0.75, -0.75)$ for Case I and $(-1.0, 1.0)$ for Case II. The remaining two settings use an extended model with two covariates

$$\log(\mu_i) = \beta_0 + \beta_1 x_{i1} + \beta_2 x_{i2}, \qquad i = 1, \ldots, n,$$

with the parameter vectors $(\beta_0, \beta_1, \beta_2)$ are $(1.5, 0.75, -0.5)$ for Case III and $(-0.5, -0.5, 1.5)$ for Case IV.

In both specifications, the covariate x_{i1} was generated from a standard normal distribution. For the two covariate models, x_{i2} was generated from a Bernoulli distribution with a success probability of 0.5. The simulation was performed for sample sizes of $n = 25, 50, 100, 150$, and 200 with 1000 replications per scenario.

Table 10. Monte Carlo simulation results for the PTS-XL regression model under Cases I and II (one-covariate cases).

Case	n	β_0					β_1				
		MSE	AAB	MRE	AL	CP	MSE	AAB	MRE	AL	CP
I	25	0.0504	0.2420	0.1815	1.1357	0.957	0.0606	0.2853	0.2140	0.9903	0.967
	50	0.0208	0.1542	0.1156	0.5873	0.944	0.0234	0.1691	0.1269	0.5574	0.974
	100	0.0172	0.1539	0.1155	0.4834	0.947	0.0129	0.1213	0.0910	0.4376	0.975
	150	0.0150	0.1203	0.0902	0.4118	0.958	0.0130	0.1108	0.0831	0.4312	0.947
	200	0.0047	0.0764	0.0573	0.2891	0.967	0.0031	0.0582	0.0437	0.2801	0.955
II	25	0.1510	0.3192	0.3192	1.8058	0.964	0.1403	0.3022	0.3022	1.5437	0.984
	50	0.0726	0.2038	0.2038	1.2471	0.984	0.0313	0.1317	0.1317	0.9461	0.925
	100	0.0435	0.1736	0.1736	0.9326	0.971	0.0244	0.1232	0.1232	0.8404	0.967
	150	0.0562	0.1817	0.1817	0.8549	0.963	0.0488	0.1770	0.1770	0.7251	0.946
	200	0.0218	0.1279	0.1279	0.5605	0.947	0.0137	0.0946	0.0946	0.5260	0.958

Table 11. Monte Carlo simulation results for the PTS-XL regression model under Cases III and IV (two-covariate cases).

Case	n	β_0					β_1					β_2				
		MSE	AAB	MRE	AL	CP	MSE	AAB	MRE	AL	CP	MSE	AAB	MRE	AL	CP
III	25	0.0294	0.0954	0.1431	0.8505	0.982	0.0368	0.2225	0.1669	0.7049	0.965	0.1581	0.6993	0.3496	2.9802	0.972
	50	0.0242	0.0869	0.1303	0.6235	0.976	0.0149	0.1283	0.0962	0.4563	0.945	0.0338	0.3075	0.1538	1.0594	0.967
	100	0.0159	0.0645	0.0967	0.5672	0.962	0.0146	0.1354	0.1015	0.4448	0.947	0.0293	0.2412	0.1206	0.9301	0.947
	150	0.0132	0.0592	0.0888	0.4507	0.944	0.0057	0.0876	0.0657	0.3189	0.945	0.0350	0.2777	0.1388	0.7239	0.981
	200	0.0127	0.0552	0.0828	0.3152	0.938	0.0047	0.0682	0.0511	0.2419	0.958	0.0207	0.2531	0.1266	0.4972	0.968
IV	25	0.2443	0.6725	0.3363	5.0871	0.892	0.0757	0.4503	0.2251	1.6603	0.947	0.3496	0.3214	0.4822	2.0861	0.892
	50	0.1032	0.4754	0.2377	1.9942	0.895	0.0397	0.2864	0.1432	0.7320	0.895	0.1118	0.1929	0.2894	1.4936	0.964
	100	0.0698	0.3740	0.1870	1.1600	0.944	0.0137	0.1740	0.0870	0.5062	0.946	0.0997	0.1675	0.2512	1.1232	0.955
	150	0.0585	0.4011	0.2005	0.9934	0.944	0.0092	0.1434	0.0717	0.4935	0.947	0.0789	0.1379	0.2069	0.9708	0.947
	200	0.0143	0.1898	0.0949	0.6374	0.963	0.0032	0.0997	0.0498	0.3160	0.972	0.0198	0.0699	0.1048	0.6741	0.947

The simulation results are reported in Tables 10 and 11. Across all scenarios, MSE, AAB, and MRE tend to decrease as the sample size increases, with some minor fluctuations observed, which are expected due to the sampling variability in Monte Carlo simulations. The AL of the confidence intervals also tends to decrease with larger sample sizes, and the CPs generally remain close to the nominal 95% level. The two covariate scenarios exhibit higher variability, particularly for the binary predictor, but this decreases as n grows. Overall, the MLEs perform reliably as the simulation results confirm the theoretical expectations.

8. Applications

This section examines the performance of the PTS-XL distribution. The distribution is compared with the Poisson distribution (P), NB distribution, the Conway–Maxwell–Poisson (COMP) distribution, the Poisson XLindley distribution (PXL) [5], the generalized Poisson (GP) distribution [36], the Poisson inverse Gaussian (PIG) distribution [37], the Poisson-Lindley (PL) distribution [2], the Poisson–new XLindley (PNXL) distribution [38], and the Poisson quasi-XLindley (PQXL) distribution [14].

8.1. Dicentric chromosome data

The first data considered in this study consists of dicentric chromosome counts observed in human peripheral blood samples with exposure to high-energy ionizing radiation. The analysis focuses on the experimental setting corresponding to a radiation dose of 1.200 gray (Gy). The observations represent the number of dicentric chromosomes per cell and have been previously analyzed in [39, 40]. A summary of the descriptive statistics is presented in Table 12. The results indicate that the data are overdispersed, with DI $>$ 1 and exceeding the mean, and exhibit positive skewness and high kurtosis. This indicates that a more flexible count model than the classical Poisson distribution is required.

Table 12. Descriptive statistics of the dicentric chromosome count data.

N	Mean	Variance	CV	DI	Skewness	Kurtosis
190	0.8579	1.1113	1.2289	1.2955	1.2828	4.3107

Table 13 summarizes the observed and expected frequencies, the MLEs with the corresponding standard errors (SEs), and goodness-of-fit measures for the competing count models. For the Pearson chi-square goodness-of-fit test, χ^2, the final categories with expected frequencies less than 5 were combined with adjacent categories. The resulting number of groups was taken as the effective number of classes, denoted k. The degrees of freedom were then calculated as $df = k - p - 1$, where p is the number of estimated parameters. The proposed PTS-XL distribution provides the best fit to the data with the lowest Akaike information criterion (AIC), Bayesian information criterion (BIC), and χ^2 values. Figure 6 supports this conclusion, as it displays the observed frequencies and the estimated PMFs of the fitted models. The PTS-XL distribution shows close alignment between the observed and expected frequencies across all count levels.

Table 13. Observed and expected frequencies, MLE, and goodness-of-fit measures for dicentric chromosome data.

X	Observed frequency	Expected frequency									
		PTS-XL	PXL	PL	PNXL	P	NB	PQXL	COMP	GP	PIG
0	92	92.9358	101.4824	99.7880	99.0702	80.5702	90.6256	91.3976	90.9462	90.3210	89.5950
1	55	55.948	47.6387	48.9467	49.9523	69.1208	58.2930	57.7176	57.3168	58.7933	59.9336
2	27	25.2083	22.1382	22.8762	23.2101	29.6492	26.0410	25.5567	26.5256	25.9884	25.9194
3	11	10.0766	10.2024	10.3512	10.2680	8.4786	9.9275	9.9025	10.2470	9.8110	9.5500
4	4	3.7695	4.6690	4.5764	4.3961	1.8184	3.4595	3.5753	3.4823	3.4158	3.3063
5	1	2.0618	3.8694	3.4615	3.1033	0.3627	1.6533	1.8502	1.4821	1.6706	1.6957
Total	190	190	190	190	190	190	190	190	190	190	190
θ	MLE	2.5188	1.3677	1.6043	1.7551	0.8579	2.5706	2.4930	0.6302	0.7437	0.8579
	SE	0.2127	0.1230	0.1408	0.1773	0.0672	1.2322	0.4834	0.0843	0.07415	0.0773
α	MLE	–	–	–	–	–	0.7498	-0.7486	0.4455	0.1332	0.4380
	SE	–	–	–	–	–	0.0915	0.1120	0.1859	0.0545	0.2374
AIC		483.001	488.623	486.944	485.909	489.815	484.72	484.892	484.303	484.875	485.270
BIC		486.248	491.870	490.191	489.156	493.062	491.215	491.386	490.797	491.369	491.764
χ^2		0.3560	4.6199	3.2887	2.5187	9.1356	0.3605	0.3684	0.1552	0.4609	0.7359
Degrees of freedom		3	3	3	3	3	3	2	1	2	2
p-value		0.9492	0.2018	0.3492	0.4719	0.0275	0.8350	0.8318	0.6936	0.7942	0.6922

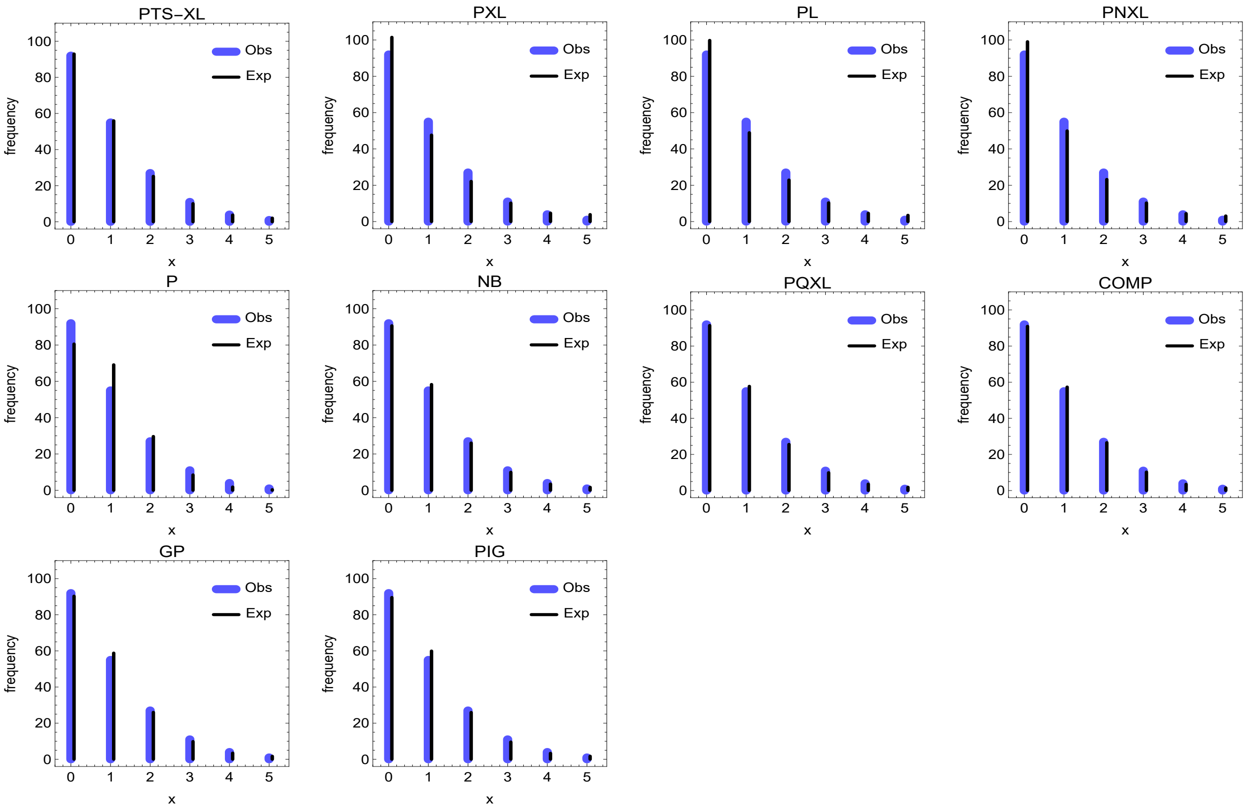

Figure 6. The estimated PMFs of the fitted distributions for dicentric chromosome data.

8.2. *Primula auricula data*

The second dataset represents the number of plants per quadrat for the species *Primula auricula* in a grassland environment. These data are commonly used in ecological studies to assess the spatial distribution of plant populations [41]. The descriptive measures summarized in Table 14 indicate that the data are overdispersed, with a DI greater than one; positively skewed; and exhibit moderate kurtosis.

Table 14. Descriptive measure for the *Primula auricula* data.

N	Mean	Variance	CV	DI	Skewness	Kurtosis
109	2.2018	4.0693	0.9162	1.8482	0.9774	3.4999

The competing models are fitted to the data and results are presented in Table 15. This table reports the observed and the corresponding expected frequencies, the estimated parameters with their standard errors, and goodness-of-fit measures. A visual comparison of the fitted models is given in Figure 7. The results show that the PTS-XL model provides the best fit, as it has the smallest AIC and BIC values among the considered models and yields the lowest χ^2 statistic with the highest associated p-value.

Table 15. Observed and expected frequencies, MLE, and goodness-of-fit measures for *Primula auricula* data.

X	Observed	Expected frequency									
	frequency	PTS-XL	PXL	PL	PNXL	P	NB	PQXL	COMP	GP	PIG
0	26	24.1251	31.9882	30.0046	31.2597	12.0554	23.5731	24.6405	24.2567	22.9304	21.7978
1	21	25.8712	23.4813	23.9348	23.8834	26.544	26.1063	25.9046	24.8015	26.6937	27.6473
2	23	20.6189	16.7957	17.7097	17.3278	29.2228	20.9436	20.3704	20.5183	21.3581	22.1515
3	14	14.4944	11.7852	12.5143	12.149	21.4479	14.6711	14.2291	14.9968	14.7091	14.8133
4	11	9.4888	8.148	8.5723	8.3135	11.8062	9.5309	9.3156	10.0388	9.3920	9.1558
5	4	5.9289	5.5675	5.7418	5.5865	5.1991	5.9007	5.8541	6.2770	5.7460	5.4739
6	5	3.5833	3.768	3.7813	3.7015	1.9079	3.5332	3.5764	3.7121	3.4256	3.2341
7	4	2.1119	2.53	2.4574	2.4251	0.6001	2.0642	2.1402	2.0943	2.0092	1.9076
8	0	1.2203	1.6875	1.5801	1.5743	0.1652	1.1835	1.2607	1.1343	1.1659	1.1285
9	1	1.5573	3.2486	2.7035	2.7793	0.0515	1.4935	1.7086	1.1701	1.5699	1.6903
Total	109	109	109	109	109	109	109	109	109	109	109
θ	MLE	1.1114	0.6217	0.7153	0.6878	2.2018	2.2282	0.9101	1.0225	1.5589	2.2018
	SE	0.0856	0.0561	0.0645	0.0728	0.1421	0.6906	0.1346	0.1455	0.1632	0.2013
α	MLE	–	–	–	–	–	0.503	-0.4785	0.3056	0.2920	0.2077
	SE	–	–	–	–	–	0.081	0.1496	0.1119	0.0613	0.0768
AIC		426.729	432.308	429.760	430.751	453.009	428.8330	428.959	427.823	429.413	430.639
BIC		429.420	434.999	432.451	433.442	455.700	434.2160	434.342	433.206	434.795	436.021
χ^2		2.4983	5.6664	3.8929	4.7126	40.9569	2.6799	2.4374	2.4324	3.0012	3.7763
Degrees of freedom		5	5	5	5	5	4	4	4	4	4
p-value		0.7768	0.3400	0.5649	0.4520	≤ 0.01	0.612743	0.6559	0.6568	0.5576	0.4371

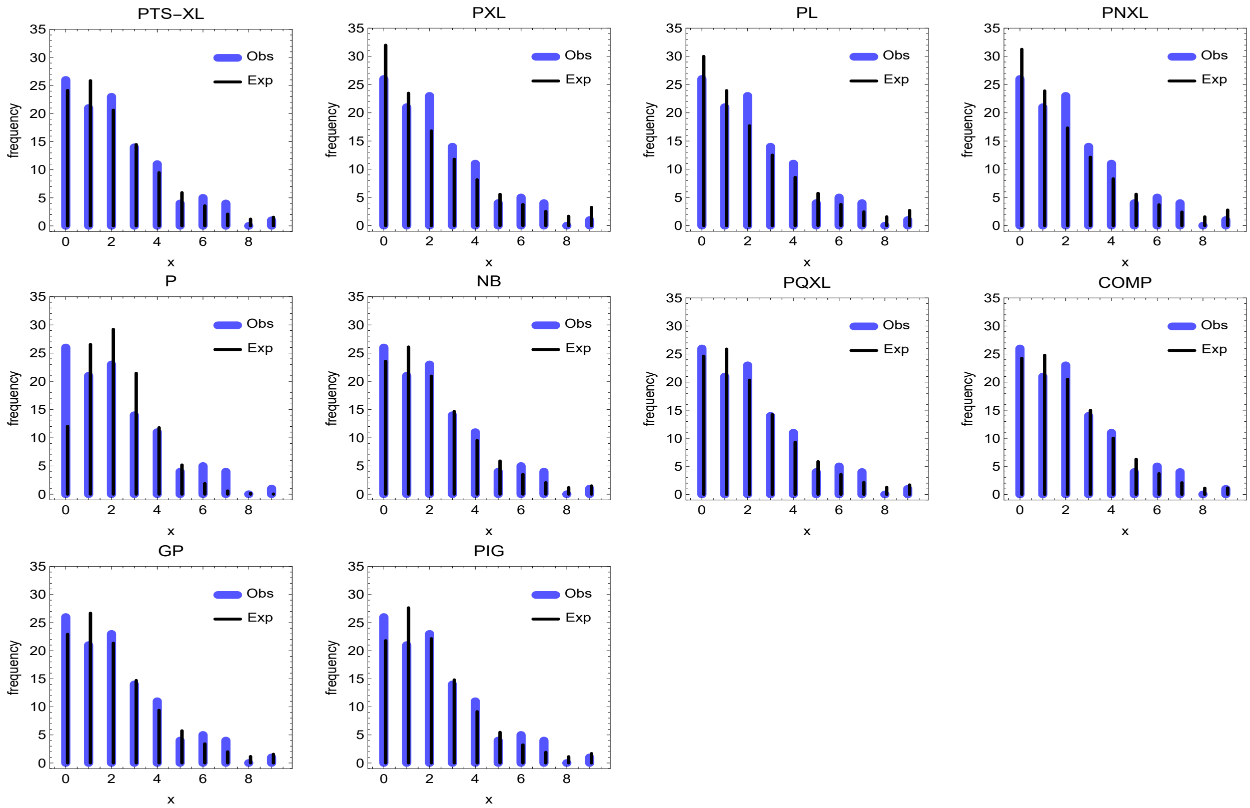

Figure 7. The estimated PMFs of the fitted distributions for *Primula auricula* data.

8.3. *Fish species data*

The third application considered originates from [42] and comprises observations from 70 lakes located in different regions of the world. The response variable is the number of fish species observed in each lake, while the explanatory variables are the lake's surface area (km^2) and the absolute latitude. Following the species–area relationship commonly used in biogeographical studies, the lake's surface area was logarithmically transformed before model fitting. This dataset is particularly suitable for assessing the performance of the proposed PTS-XL regression model due to the pronounced overdispersion present in the species counts, with a sample mean of 15.33 and a variance of 329.99. The parameter estimates obtained from the PTS-XL, PL, P, and NB regression models are given in Table 16.

In the results in Table 16, the regression coefficients are highly significant across all fitted models, indicating that larger lakes tend to contain more fish species, whereas species richness decreases with increasing latitude. The PTS-XL regression model has the lowest AIC and BIC values among the fitted models. However, the AIC values of the PTS-XL and NB regression models are very close, with only a slight advantage in favor of the PTS-XL model; the lower BIC value of the PTS-XL model, together with its fewer parameters, suggests that it can provide a useful alternative for modeling count data such as the fish species data.

Table 16. MLE, AIC, and BIC for fitted regression models for fish species data.

Covariates	PTS-XL			PL			P			NB		
	Estimate	SE	p-value	Estimate	SE	p-value	Estimate	SE	p-value	Estimate	SE	p-value
β_0	1.7166	0.3050	<0.0001	1.7146	0.3752	<0.0001	1.6801	0.1255	<0.0001	1.7092	0.2984	<0.0001
β_1	0.2307	0.0396	<0.0001	0.2298	0.0496	<0.0001	0.2475	0.0146	<0.0001	0.2303	0.0395	<0.0001
β_2	-0.0184	0.0044	<0.0001	-0.0181	0.0053	<0.0001	-0.0212	0.0018	<0.0001	-0.0181	0.0042	<0.0001
AIC		482.559			489.078			722.678			482.701	
BIC		489.305			495.823			729.424			491.695	

To further assess the adequacy of the fitted PTS-XL regression model, a comprehensive residual diagnostic analysis is presented in Figure 8. This figure presents diagnostic plots for the fitted PTS-XL regression model. The RQR Q–Q plot shows that the points lie reasonably close to the reference line, while the RQR, Pearson, and deviance residuals are generally scattered around zero without clear systematic patterns. The leverage plot also shows relatively small leverage values for most observations. Furthermore, the Pearson chi-square statistic is 59.1196 with 67 degrees of freedom and a p-value of 0.7426. Thus, there is no evidence of lack of fit. Overall, these results support the adequacy of the PTS-XL regression model for the fish species data.

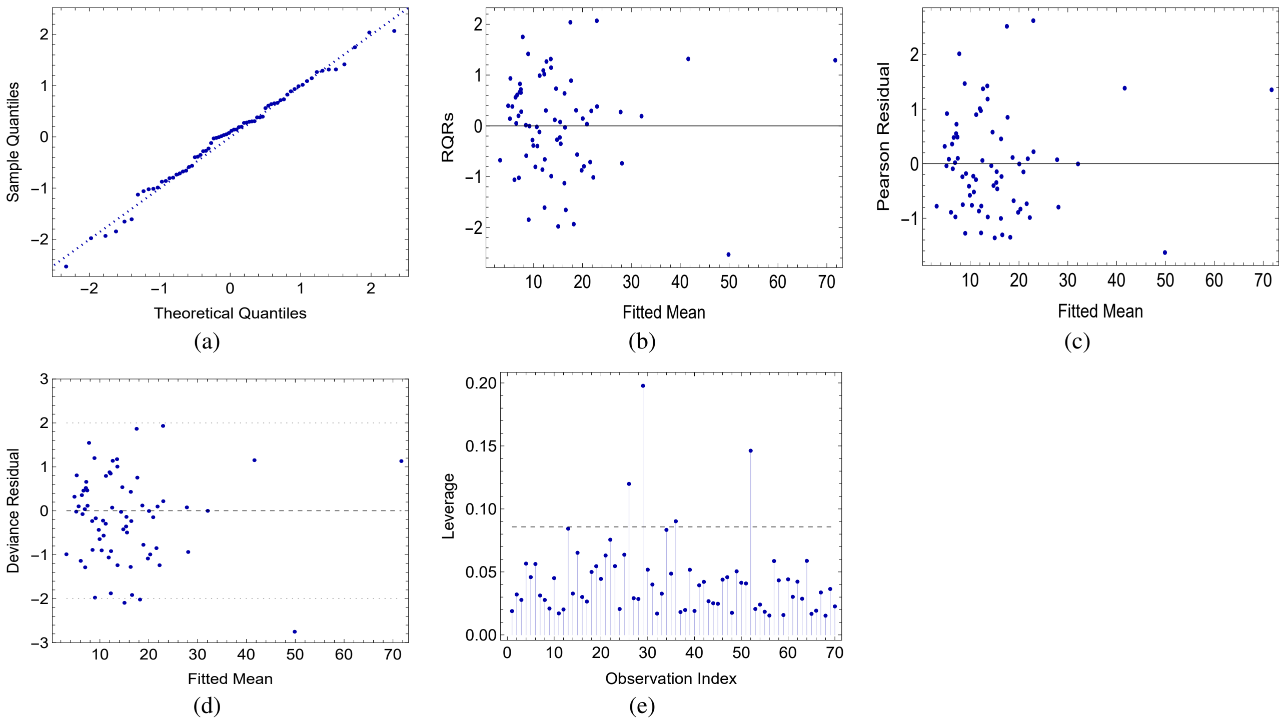

Figure 8. Diagnostic plots for the fitted PTS-XL regression model for the fish species data. (a) Normal Q–Q plot of the RQRs; (b) RQRs versus fitted mean; (c) Pearson residuals versus fitted mean; (d) deviance residuals versus fitted mean; and (e) leverage diagnostics.

9. Conclusions

This paper proposed a new one-parameter count distribution, called the PTS-XL distribution, by compounding the Poisson distribution with a TS-XL distribution. The TS-XL distribution is obtained as the sum of two independent XLindley random variables, providing a more flexible mixing distribution by introducing additional variability while preserving a simple one-parameter structure. Several properties of the PTS-XL distribution were derived, including its distributional characteristics, moments, generating functions, and stress–strength reliability. The PTS-XL distribution exhibits tractable mathematical properties and is capable of modeling overdispersed, moderately dispersed, and equidispersed count data. Three classical estimation methods were developed for estimating the model's parameter and were assessed through an extensive Monte Carlo simulation study. A further contribution of this work is the development of a count regression model based on the PTS-XL distribution. The regression parameters were estimated using the maximum likelihood method, and their performance was assessed via Monte Carlo simulation. The practical usefulness of both the proposed distribution and the regression model was demonstrated using real data applications, in which the proposed model consistently outperformed several well-established competing count models. These findings indicate that the PTS-XL distribution provides flexibility and effective alternative for modeling equidispersed and overdispersed count data. Future research may consider zero-inflated, hurdle, multivariate, and time-series extensions of the proposed distribution.

Author contributions

Mahmoud M. El-Awady: Conceptualization, methodology, software, formal analysis, writing original draft preparation, project administration; Hanan Haj Ahmad: Validation, investigation, formal analysis, writing review and editing, visualization, funding acquisition. All authors have read and agreed to the published version of the manuscript.

Use of Generative-AI tools declaration

The authors declare that they have not used Artificial Intelligence (AI) tools in the creation of this article.

Funding

This work was supported by the Deanship of Scientific Research, Vice Presidency for Graduate Studies and Scientific Research, King Faisal University, Saudi Arabia (Grant No. KFU264776).

Conflict of interest

The authors declare that they have no conflicts of interest.

References

1. D. Karlis, E. Xekalaki, Mixed poisson distributions, *Int. Stat. Rev.*, 2005, 35–58.
2. M. Sankaran, 275. note: The discrete poisson-lindley distribution, *Biometrics*, 1970, 145–149. https://doi.org/10.2307/2529053
3. E. Bereta, F. Louzanda, M. Franco, The poisson-weibull distribution, *Adv. Appl. Stat.*, **22** (2011), 107–118.
4. R. Grine, H. Zeghdoudi, On poisson quasi-lindley distribution and its applications, *J. Mod. Appl. Stat. Meth.*, **16** (2017), 21. https://doi.org/10.22237/jmasm/1509495660
5. M. Ahsan-ul Haq, A. Al-Bossly, M. El-Morshedy, M. S. Eliwa, Poisson xlindley distribution for count data: Statistical and reliability properties with estimation techniques and inference, *Computat. Intel. Neurosc.*, **2022** (2022), 6503670.
6. E. Altun, G. M. Cordeiro, M. M. Ristić, An one-parameter compounding discrete distribution, *J. Appl. Stat.*, **49** (2022), 1935–1956. https://doi.org/10.1080/02664763.2021.1884846
7. F. Seghier, M. Ahsan-ul Haq, H. Zeghdoudi, S. Hashmi, A new generalization of poisson distribution for over-dispersed, count data: Mathematical properties, regression model and applications, *Lobachevskii J. Math.*, **44** (2023), 3850–3859. https://doi.org/10.1134/S1995080223090378
8. T. N. Sindhu, Y. El Khatib, T. A. Abushal, A. S. Alharthi, Modeling biological count data with the poisson-mgamma distribution: Applications to radiation and yeast cell analysis, *Results Eng.*, **29** (2026), 109193. https://doi.org/10.1016/j.rineng.2026.109193
9. M. Shoukri, M. Asyali, R. VanDorp, D. Kelton, The poisson inverse gaussian regression model in the analysis of clustered counts data, *J. Data Sci.*, **2** (2004), 17–32. https://doi.org/10.6339/JDS.2004.02(1).135
10. D. Lord, S. R. Geedipally, The negative binomial–lindley distribution as a tool for analyzing crash data characterized by a large amount of zeros, *Accident Anal. Prev.*, **43** (2011), 1738–1742. https://doi.org/10.1016/j.aap.2011.04.004
11. L. Cheng, S. R. Geedipally, D. Lord, The poisson–weibull generalized linear model for analyzing motor vehicle crash data, *Safety Sci.*, **54** (2013), 38–42. https://doi.org/10.1016/j.ssci.2012.11.002
12. H. Zamani, N. Ismail, P. Faroughi, Poisson-weighted exponential univariate version and regression model with applications, *J. Math. Stat.*, **10** (2014), 148. https://doi.org/10.3844/jmssp.2014.148.154
13. W. Wongrin, W. Bodhisuwan, Generalized poisson–lindley linear model for count data, *J. Appl. Stat.*, **44** (2017), 2659–2671. https://doi.org/10.1080/02664763.2016.1260095
14. F. M. Alghamdi, M. Ahsan-ul Haq, M. N. S. Hussain, E. Hussam, E. M. Almetwally, H. M. Aljohani, et al., Discrete poisson quasi-xlindley distribution with mathematical properties, regression model, and data analysis, *J. Radiat. Res. Appl. Sc.*, **17** (2024), 100874.
15. R. A. Ahmed, Z. Y. Algamal, L. A. Mohamud, A poisson-modified quasi-lindley regression approach for multicollinear data using kibria–lukman estimator, *Sci. Afr.*, **33** (2026), e03465. https://doi.org/10.1016/j.sciaf.2026.e03465

16. D. V. Lindley, Fiducial distributions and bayes' theorem, *J. Roy. Stat. Soc. B*, **20** (2018), 102–107. https://doi.org/10.1111/j.2517-6161.1958.tb00278.x
17. S. Chouia, H. Zeghdoudi, The xlindley distribution: properties and application, *J. Stat. Theory Appl.*, **20** (2021), 318–327. https://doi.org/10.2991/jsta.d.210607.001
18. S. Mohan, R. Moharana, K. Maiti, On record-based transmuted x-lindley distribution: Properties and applications, *J. Dyn. Games*, 2026. https://doi.org/10.3934/jdg.2026011
19. M. M. El-Awady, H. H. Ahmad, Y. Rabaiah, A. T. Ramadan, The q-deformed lindley distribution: Properties, statistical inference, and applications, *Mathematics*, **14** (2026), 1364. https://doi.org/10.3390/math14081364
20. A. M. Gemeay, A. Ezzebsa, H. Zeghdoudi, C. Tanış, Y. A. Tashkandy, M. Bakr, et al., The power new xlindley distribution: Statistical inference, fuzzy reliability, and applications, *Heliyon*, **10** (2024), e36594. https://doi.org/10.1016/j.heliyon.2024.e36594
21. A. Haddari, H. Zeghdoudi, R. Pakyari, A new two-parameter family of discrete distributions, *Heliyon*, **11** (2025), e41459. https://doi.org/10.1016/j.heliyon.2024.e41459
22. C. Chesneau, L. Tomy, J. Gillariose, On a sum and difference of two lindley distributions: Theory and applications, *REVSTAT-Stat. J.*, **18** (2020), 673–695.
23. C. Chesneau, V. D'cruz, R. Maya, M. Irshad, A novel discrete distribution based on the mixture of poisson and sum of two lindley random variables, *REVSTAT-Stat. J.*, **23** (2025), 371–396.
24. M. R. Irshad, C. Chesneau, V. D'cruz, N. M. Khan, R. Maya, Bivariate Poisson 2Sum-Lindley distributions and the associated BINAR(1) processes, *Mathematics*, **10** (2022), 3835. https://doi.org/10.3390/math10203835
25. J. Keilson, H. Gerber, Some results for discrete unimodality, *J. Am. Stat. Assoc.*, **66** (1971), 386–389. https://doi.org/10.1080/01621459.1971.10482273
26. P. L. Gupta, R. C. Gupta, R. C. Tripathi, On the monotonic properties of discrete failure rates, *J. Stat. Plan. Infer.*, **65** (1997), 255–268. https://doi.org/10.1016/S0378-3758(97)00064-5
27. A. W. Kemp, Classes of discrete lifetime distributions, *Commun. Stat.-Theor. M.*, **33** (2004), 3069–3093. https://doi.org/10.1081/STA-200039051
28. F. W. Olver, *NIST handbook of mathematical functions hardback and CD-ROM*, Cambridge university press, 2010. https://doi.org/10.1109/TR.2025.3647489
29. D. Zhu, A. Xu, Z. Chen, S. Ding, G. Fang, An online bayesian framework for identifying latent system degradation states, *IEEE T. Reliab.*, **75** (2026), 542–554. https://doi.org/10.1109/TR.2025.3647489
30. A. Xu, Z. Chen, H. Yin, Y. Tang, A bivariate wiener degradation model with partially random scale weights, *Reliab. Eng. Syst. Safe.*, **275** (2026), 112684. https://doi.org/10.1016/j.ress.2026.112684
31. A. Xu, Y. Miao, J. Sun, S. Zhou, Y. Tang, A hierarchical bayesian multivariate wiener process model with dependent degradation rates and volatilities, *IEEE T. Reliab.*, **75** (2026), 1420–1433. https://doi.org/10.1109/TR.2026.3674703
32. R. J. Tibshirani, B. Efron, *An introduction to the bootstrap*, Boca Raton, Florida, 2000.
33. W. Rudin, *Principles of mathematical analysis*, 3 Eds., New York: McGraw-Hill, 1976.

34. P. K. Dunn, G. K. Smyth, Randomized quantile residuals, *J. Comput. Graph. Stat.*, **5** (1996), 236–244. https://doi.org/10.1080/10618600.1996.10474708

35. J. W. Hardin, J. M. Hilbe, *Generalized linear models and extensions*, Stata Press, 2007.

36. P. C. Consul, G. C. Jain, A generalization of the poisson distribution, *Technometrics*, **15** (1973), 791–799. https://doi.org/10.1080/00401706.1973.10489112

37. G. E. Willmot, The poisson-inverse gaussian distribution as an alternative to the negative binomial, *Scand. Actuar. J.*, **1987** (1987), 113–127. https://doi.org/10.1080/03461238.1987.10413823

38. M. Vardaki, H. Papageorgiou, Poisson quasi-lindley and poisson-new xlindley univariate and bivariate models: Derivation techniques and automobile insurance applications, *AIMS Math.*, **11** (2026), 3772–3810. https://doi.org/10.3934/math.2026154

39. M. Di Giorgio, A. A. Edwards, J. Moquet, P. Finnon, P. Hone, D. Lloyd, et al., Chromosome aberrations induced in human lymphocytes by heavy charged particles in track segment mode, *Radiat. Prot. Dosim.*, **108** (2004), 47–53. https://doi.org/10.1093/rpd/nch012

40. P. Puig, J. F. Barquinero, An application of compound poisson modelling to biological dosimetry, *Pro. Roy. Soc. A-Math. Phys.*, **467** (2011), 897–910. https://doi.org/10.1098/rspa.2010.0384

41. C. I. Bliss, R. A. Fisher, Fitting the negative binomial distribution to biological data, *Biometrics*, **9** (1953), 176–200. https://doi.org/10.2307/3001850

42. C. D. Barbour, J. H. Brown, Fish species diversity in lakes, *Am. Nat.*, **108** (1974), 473–489. https://doi.org/10.1086/282927